Design and analysis of Photonic Crystal Fiber with Large Negative Dispersion and Small Dispersion Slope

Thesis submitted in the partial fulfillment of requirement for the award of degree of

Master of Engineering

in

Electronics and Communication Engineering

Submitted by:

Rahul Singh

Roll No : 801061032

Under the guidance of:

Dr. Mukesh Kumar

Assistant Professor

ELECTRONICS AND COMMUNICATION ENGINEERING DEPARTMENT

THAPAR UNIVERSITY

(Established under the section 3 of UGC Act, 1956)

PATIALA – 147004 (PUNJAB)

DECLARATION

I, Rahul Singh, hereby certify that the work which is being presented in this thesis entitled "Design and Analysis of Photonic Crystal Fiber with Large Negative Dispersion and Small Dispersion Slope" by me in partial fulfillment of the requirements for the award of degree of Master of Engineering in Electronics and Communication Engineering from Thapar University (Deemed University), Patiala, is an authentic record of my own work carried out under the supervision of Dr. Mukesh Kumar.

The matter presented in this thesis has not been submitted in any other University / Institute for the award of any other degree.

Date: 02/07/12

Rahul Singh
Roll No: 801061032

It is certified that the above statement made by the student is correct to the best of my knowledge and belief.

Date: 2/7/2012

Dr. Mukesh Kumar
Assistant Professor
ECED

Countersigned by:

(Dr. Rajesh Khanna)
Professor and Head ECED
Thapar University, Patiala
Date:

(Dr. S.K. Mohapatra)
Dean of Academic Affairs
Thapar University, Patiala
Date:

ACKNOWLEDGEMENT

I would like to express my special thanks and deep sense of gratitude to my Thesis Adviser, **Dr. Mukesh Kumar,** Asst. Professor, Electronics & Communication Engineering Department, Thapar University, Patiala for their continuous indefatigable guidance which paved me on to the path to carry this thesis within time. I am highly indebted to them for their painstaking efforts and invaluable suggestions during the period of work.

I take this opportunity to express my gratitude and sincere thanks to **Dr. Rajesh Khanna**, Professor and Head , **Dr. Kulbir Singh**, Associate Professor of Electronics & Communication Engineering Department for their valuable advice and suggestion and for providing me the opportunity to complete my thesis work .

I would also like to thank all the staff members of Electronics & Communication Engineering Department for providing me all the facilities required for the completion of this work.

Date: 02/07/12

Rahul

(Rahul Singh)

Place: Patiala

ii

ABSTRACT

Conventional optical fibers can only guide light in a high refractive index core by total internal reflection. By using total internal reflections, it is not possible to guide light in an air core. Light guidance in air is of great interest for various technological and scientific applications and has only recently been possible with the advent of photonic band gap fibers. Control of dispersion in PCFs is very important problem for realistic applications of optical fiber communications, dispersion compensation and nonlinear optics. Usually the positive dispersion of the optical fiber, which is a major factor to cause optical pulse broadening and restrict transmission distance and bandwidth, can be compensated by using dispersion compensating fiber (DCF) with large negative dispersion.

The present work aims at the designing and simulation of a structure with ultra-flattened dispersion, low modal birefringence and low polarization dependent loss single mode photonic crystal fibers. By varying various parameters such as diameter of air holes (d), number of air holes rings (N), refractive index of cladding (n), hole pitch (Λ) analysis has been done for an optimum profile. Although the largest negative dispersion value of -31.6 ps/nm/km is calculated for d= .44μm but desired structure has been achieved with d= .42μm, N = 8, n = 1.4, Λ = 1.5μm low ultra flattened dispersion in a range of -20.35 to –20.12ps/nm/km with dispersion slope equal to -5.47×10^{-4} ps/nm/km within the wavelength range of 1.49 to 1.91 μm. Low modal birefringence on the order of 10^{-4} and low polarization dependent loss on the order of 10^{-14} is realized with the proposed PCF structure.

TABLE OF CONTENTS

LIST OF TABLES

LIST OF FIGURES

Chapter 1

Introduction

1.1 Background and motivation of Photonic crystal fiber

The fact that modern optical fibers transmit information over long distances at extremely high speed rates is a truly fantastic technological and scientific achievement of the last century. Every day we all use optical fibers when making telephone calls, connecting to the internet, and reading our e-mails. Currently, optical fibers are increasingly been used in non telecommunications applications such as: structural sensing, biomedicine, medical imaging, astronomy and micro-machining, among many other fields. Conventional optical fibers are formed from two different glasses. One with a higher refractive index runs down the middle of the fiber, forming the core in which light is trapped. A second lower-index glass surrounds the inner rod, protecting it and forming the cladding of the fiber. The inner rod has to have a higher refractive index than the outer, because only then light can be guided in the core by total internal reflections at the core-cladding boundary. Recently, a novel type of optical fibers was envisioned by Philip Russell [1- 2]. These new fibers, known as photonic crystal fibers, can be made entirely from a single material as they do not rely on dopants for light guidance. Instead, the cladding region in photonic crystal fibers has wavelength-scale holes running down the fiber length. The discovery of photonic crystal fibers has been very promising for optical fiber technology since they have enabled light to be controlled in ways not previously possible or even imaginable with conventional optical fiber technology [2].

Research on single material fibers dates back to the early years of fiber optics in the 1970's. At that time, Kaiser et al. [3-4] fabricated a single material fiber consisting of a small diameter silica rod supported by thin struts inside a large tube, Fig. 1.1a. Their motivation was to overcome the difficulties in having different chemical compositions required for the core and cladding materials. The development of chemical vapour deposition (CVD) for optical fiber fabrication also in the 1970's overcame such negative effects providing high purity ultra-low loss synthetic silica [5-6]. CVD also permitted to precisely control the refractive index of silica by the introduction of index increasing dopants (germanium, aluminium) and index decreasing dopants (boron, fluorine)[7-8]. The promising capabilities

of CVD for making single-mode low-loss optical fibers [9] left single-material fibers research aside for many years. Russell's idea of light guidance in a hollow-core by surrounding it with a large number of smaller holes in order to form a synthetic material which would trap light by using a photonic band gap renewed the interest in single material optical fibers [1, 10-11]. The fabrication of an only-silica photonic crystal fiber in 1996 by Knight et al. [12] containing hundreds of air channels of micrometer dimensions forming a two-dimensional photonic crystal around a silica core, Fig. 1.1(b), which was single mode over a very wide spectral range, led to the discovery of endlessly single-mode PCFs by Birks et al. [13]. This seminal work in photonic crystal fibers fueled the ambition that they would support the growing demands on the performance and functionality of optical fibers. The unusual modal properties of this fiber burst the activities on photonic crystal fiber research.

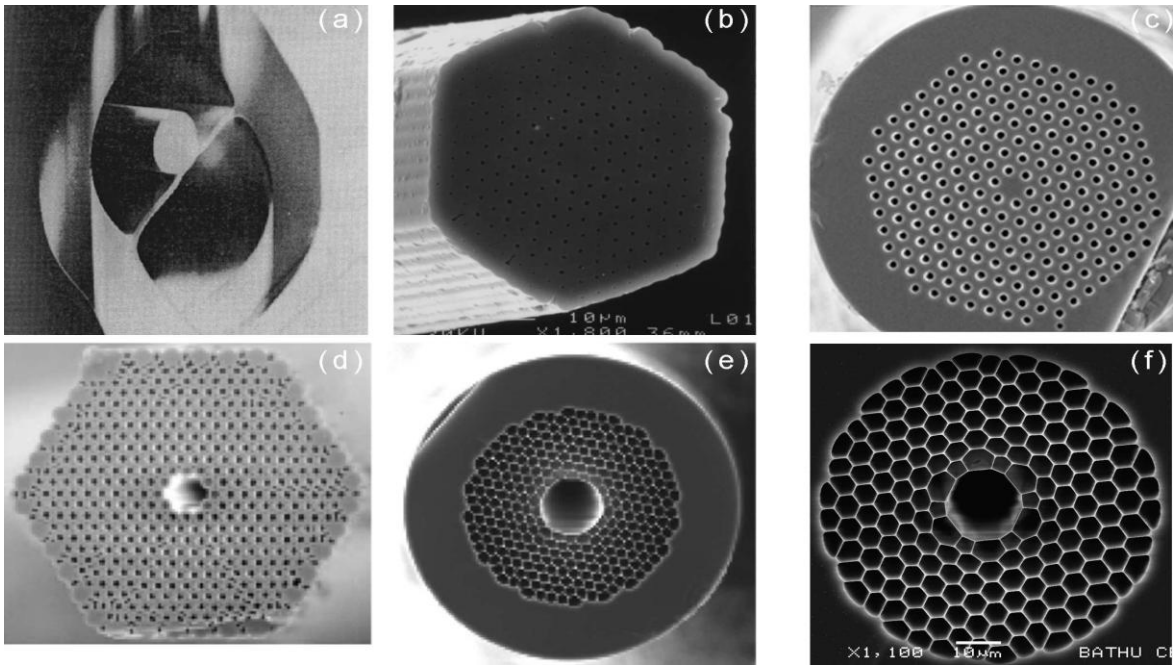

Fig. 1.1: Examples of index guiding PCFs (top) and photonic band gap fibers (bottom). (a) First demonstration of a silica-only fiber by Kaiser et al. in 1973 [3]. (b) Scanning electron microscope (SEM) image of the first photonic crystal fiber with a silica core surrounded by a periodic array of air holes in silica by Knight et al. in 1996 [12]. (c) Endlessly single-mode PCF fabricated at the ORC. (d) SEM micrograph of the first hollow-core PCF by Cregan et al. in 1999 [14]. (e) SEM micrograph of the lowest loss hollow-core band gap fiber by Blaze photonics [15]. (f) Hollow-core PCF by Amezcua et al. in 2008 [16].

1.2 Classification of photonic crystal fibers depending on their guidance mechanism

There are two major classes of photonic crystal fibers depending on their guidance mechanism: index guiding photonic crystal fibers, which guide light due to a "reduced" refractive index of the cladding region and photonic band gap fibers, which confine light thanks to photonic band gaps formed by the cladding. Although fibers belonging to these two classes have been fabricated of different materials and with several cladding configurations, the fibers of interest for this work have a two-dimensional photonic crystal cladding formed by an array of air holes in silica that run down the full fiber length, Fig. 1.1.

Index-guiding PCFs consist of a solid core surrounded by an array of air holes, Fig. 1.1(b) (c). In this case, the air holes can be seen as to lower the effective refractive index of the cladding region as compare to that of the solid core and guidance occurs by a modified total internal reflection mechanism. Although this mechanism is similar to the way in which conventional optical fibers guide light, the wavelength scale features of the fiber lead to a strongly wavelength dependent cladding index leading to a host of unusual optical properties unique to photonic crystal fibers, including single-mode guidance at all wavelengths and striking nonlinear and dispersive properties[1, 2, 12, 17-20].

In contrast to index guiding PCFs, in which the guidance mechanism is conceptually similar to that of conventional fibers, photonic band gap fibers guide light by a completely radical concept: photonic band gap effects. In photonic band gap fibers the air holes that define the cladding region have to be arranged in a highly perfect periodical lattice. For certain geometries, the cladding can then form two-dimensional photonic band gaps which prohibit the propagation of light for specific frequencies and propagation constant values [10]. By breaking the order of the cladding (adding a defect in the periodic structure), it is possible to introduce localized modes within the defect. This is typically done by introducing a bigger hole at the centre of the structure. If light can propagate in the defect but its frequency lies within a band gap it will not be allowed to propagate in the cladding and therefore the optical energy will be concentrated in the core and guided with low-loss. Hollow-core photonic band

gap fibers (HC-PBGFs) are a special class of band gap fibers that guide light in an air core. In 1999, Cregan et al. [14] demonstrated the first HC-PBGF and over the past decade they have been developed to high-performance products, Fig. 1.1. Indeed, now fibers with very low attenuation-well below than 20dB/km at 1550 nm wavelength- are readily available and the best loss value in a hollow-core fiber is only 1.2 dB/km [15] which is around 10 times higher than the minimum attenuation of ~0.15 dB/km in conventional fibers.

1.3 Recent work

Until recently, an optical fiber was a solid thread surrounded by another material with a lower refractive index. Today the photonic crystal fibers (PCFs) are established as an alternative fiber technology. PCFs, which have been first demonstrated in 1995, are optical fibers with a periodic arrangement of low-index material in a background with higher refractive index. The background material in PCFs is usually undoped silica and the low index region is typically provided by air-holes running along their entire length. Two main categories of PCFs exist: high-index guiding fibers and photonic band gap ones. PCFs belonging to the first category are more similar to conventional optical fibers, because light is confined in a solid core by exploiting the modified total internal reflection mechanism. In fact, there is a positive refractive index difference between the core region and the photonic crystal cladding, where the air-hole presence causes a lower average refractive index. The guiding mechanism is defined as "modified" because the cladding refractive index is not a constant value as in standard optical fibers but it changes significantly with the wavelength. This characteristic as well as the high refractive index contrast between silica and air provides a range of new interesting features. Moreover, high design flexibility is one of the distinctive properties of PCFs. In particular, by changing the geometric characteristics of the air-holes in the fiber cross-section, that is, their dimension or position, it is possible to obtain PCFs with diametrically opposite properties. For example, PCFs with a small silica core and large air-holes, that is, with a high air-filling fraction in the transverse section have better nonlinear properties compared with conventional optical fibers and so they can be successfully used in many applications, like super continuum generation.

On the contrary fibers can be designed with small air-holes and large hole-to-hole distances in order to obtain a large modal area, useful for high power delivery. Differently from

standard fibers PCFs with proper geometric characteristics can be endlessly single mode, that is, only the fundamental mode is guided regardless of the wavelength. In addition a significant asymmetry can be introduced in a simple way in the PCF core, thus creating fibers with very high level of birefringence. Moreover the PCF dispersion properties can be tailored with high flexibility so that it is possible to move the zero-dispersion wavelength to the visible range as well as to obtain dispersion curves ultra flattened or with a strong negative slope [21- 23].

When the PCF core region has a lower refractive index than the surrounding photonic crystal cladding, light is guided by a mechanism different from total internal reflection – by exploiting the presence of the photonic band gap (PBG). In fact, the air-hole microstructure which constitutes the PCF cladding is a two-dimensional photonic crystal that is a material with periodic dielectric properties characterized by a photonic band gap, where light in certain wavelength ranges cannot propagate. The PBG effect can be also found in nature since it is responsible, for example, of the beautiful and bright colors seen in butterfly wings. PCFs with a low index core are created by introducing a defect in the photonic crystal structure, for example, an extra air-hole or an enlarged one, and light is confined because the PBG makes propagation in the micro structured cladding region impossible [24]. This guiding mechanism cannot be obtained in conventional optical fibers and it opens a whole new set of interesting possibilities. In particular, light can be guided in air in PCFs with a hollow core thus providing numerous promising applications such as low-loss guidance and high-power delivery without the risk of fiber damage. Moreover air-guiding PCFs are almost insensitive to bending even for small bending diameter values and they present extreme dispersion properties, highly dominated by the waveguide component. Finally, when filled with proper gases or liquids, hollow core PCFs can be successfully employed in sensor applications or for nonlinear optics.

One of the most important advantages offered by photonic crystal fibers (PCFs) is the high design flexibility. In fact, by changing the geometric characteristics of the fiber cross-section such as the air-hole dimension or disposition, it is possible to obtain fibers with diametrically opposed optical properties. PCFs with unusual guiding, dispersion and nonlinear properties can be designed and successfully used in various applications as reported in this section.

The main drawback which affects this new kind of fibers is related to the attenuation, which is higher than that of conventional optical fibers. The different loss mechanisms are thus analyzed for both solid- and hollow-core photonic crystal fibers. In general, a loss reduction for PCFs can be obtained by improving the fabrication process, reported in the last part of the chapter. The stack-and draw process is described with other fabrication techniques [25]. Once reached the technological maturity, the advantages offered by PCFs with respect to conventional fibers could be completely exploited for different applications and the new fibers will enter concretely in the market.

1.4 Aim and outlines of thesis

The present work aims at the designing a structure with ultra-flattened dispersion, low modal birefringence and low polarization dependent loss, single mode silica air photonic crystal fibers.

In this work, various parameters are varied such as diameter of air holes(d), number of air holes rings(N), refractive index of cladding(n), hole pitch(Λ) analysis has been done for an optimum profile design. The simulation is done using eigenmode expansion method and the results are validated with Finite Difference Method (FDM) using Lumerical Mode Solution (LMS).

Chapter 2 provides an introduction to photonic crystal fibers, including a description of the stack and draw technique used for the fabrication of silica photonic crystal fibers. It also includes a comprehensive description of the optical properties of photonic crystals and the optical properties of index-guiding PCFs are briefly discussed.

Chapter 3 discussed about the research work done in the photonic crystal fibers.

Chapter 4 discussed the design and simulation a structure of photonic crystal fiber with controlling of dispersion, modal birefringence and polarization dependent loss.

Chapter 2

Photonic Crystal Fibers: introduction and recent advances

It is important to mention that photonic crystal fibers are also referred as microstructured optical fibers and holey fibers. In a conventional optical fiber the light propagation is due to total internal reflection at the core/cladding interface. In contrast to this, PCFs are able to guide light by means of two different mechanisms: Modified total internal reflection, in which light is guided in a solid core, surrounded by a (not necessarily periodic) structured cladding. In this case the average refractive index of the cladding is decreased because of the air holes (low refractive index) [12]. On the other hand, photonic band gap fibers exploit two dimensional photonic band gaps as the mechanism of light guidance therefore they can guide light in a low refractive index medium [10, 14, 25]. In photonic band gap fibers the air holes that define the cladding region are arranged in a periodic lattice which presents a photonic band gap that does not allow light to propagate in the cladding region under certain conditions.

A good starting point for understanding the properties of photonic crystal fibers is that of photonic crystals. This chapter gives an insight into photonic crystal and the formation of photonic band gaps. A comprehensive review of the optical properties, guidance mechanisms and fabrication methods of photonic crystal fibers is also presented here.

2.1 Fundamentals of photonic crystals

The periodic structure of atoms within a conducting medium gives rise to different electronic bands, allowing the control of the propagation of electrons through the material [26-27]. This has been understood for many years, and ultimately has led to personal computers. However, it was not until 1987 when Yablonovitch [28] and John [29] proposed an analogous system to control the propagation of light. The optical version of a solid state crystal, a photonic crystal, is made from dielectric materials periodically patterned on the wavelength scale. Photonic crystals were predicted theoretically to describe two new optical principles, the localization and trapping of light [29-30] and the complete inhibition of spontaneous emission [28]. In photonic crystals the periodical refractive index distribution can give rise to

bandgaps in the dispersion relations of Electromagnetic waves. Then propagation of light within these bandgaps is forbidden and thus photonic crystals allow for a fine degree of control over the optical field within a material giving new opportunities in quantum optics, optoelectronics and nonlinear optics [31].

2.1.1 Theoretical description of photonic crystals

The basic starting point in understanding the optical properties of photonic crystals is that of Maxwell's equations. An electromagnetic wave can be expressed in terms of an electric field vector $\vec{E}$ and a magnetic field vector $\vec{B}$. When incident on a material the terms $\vec{H}$, the magnetic flux density $\vec{D}$, the electric displacement vector $\overrightarrow{J_{free}}$, the current density and ρ_{free} the charge density are also defined. The Maxwell's equations in the differential form may be expressed in the International System units as:

$$\nabla \times \vec{E}(\vec{r},t) = -\partial \vec{B}(\vec{r},t)/\partial t \quad (2.1a)$$

$$\nabla \times \vec{H}(\vec{r},t) - \partial \vec{D}(\vec{r},t)/\partial t = \overrightarrow{J_{free}} \quad (2.1b)$$

$$\nabla . \vec{B}(\vec{r},t) = 0 \quad (2.1c)$$

$$\nabla . \vec{D}(\vec{r},t) = \rho_{free} \quad (2.1d)$$

Considering a number of assumptions valid for our particular case the previous equations can be simplified. First, for a medium that is free of free charges and free currents, ρ_{free} and $\overrightarrow{J_{free}}$ are set to zero. Next, if the field strengths are assumed to be small enough, the relations $\vec{D}$ to $\vec{E}$ and $\vec{B}$ to $\vec{H}$ can be consider as linear. Finally, for isotropic loss-less materials the dielectric permittivity, $\varepsilon(\vec{r},\omega)$, is scalar and real; where $\vec{r}$ is the spatial vector and ω is the angular frequency of light. Then, the constitutive equations of the material are given by:

$$\vec{D}(\vec{r},t) = \varepsilon(\vec{r})\vec{E}(\vec{r},t) \quad (2.2a)$$

$$\vec{B}(\vec{r},t) = \mu_0 \vec{H}(\vec{r},t) \quad (2.2b)$$

Where, μ_0 is the magnetic permeability of vacuum. If harmonic time dependence of the electromagnetic fields is assumed, the fields can be written as,

$$\vec{E}(\vec{r},t) = \vec{E}(\vec{r})e^{i\omega t} \quad (2.3)$$

$$\vec{H}(\vec{r},t) = \vec{H}(\vec{r})e^{i\omega t}$$

By the substitution of equations (2.2) into equations (2.1) the following system is obtained :

$$\nabla \times \vec{E}(\vec{r}) = -i\omega\mu_0 \vec{H}(\vec{r}) \quad (2.4a)$$

$$\nabla \times \vec{H}(\vec{r}) = i\omega\varepsilon(\vec{r})\vec{E}(\vec{r}) \quad (2.4b)$$

$$\nabla . \vec{H}(\vec{r}) = 0 \quad (2.4c)$$

$$\nabla . \varepsilon(\vec{r})\vec{E}(\vec{r}) = 0 \quad (2.4d)$$

Equation (2.4a) and equation (2.4b) can be rearranged into a single vectorial expression satisfied by the magnetic field $\vec{H}(\vec{r})$

$$\nabla \times \left(\frac{1}{\varepsilon(\vec{r})}\nabla \times \vec{H}(\vec{r})\right) = \omega^2\mu_0\vec{H}(\vec{r}) \quad (2.5)$$

This general expression represents an eigenvalue problem that together with the divergence equation (2.4c) govern the response of an optical field in a dielectric medium whose dielectric constant distribution is given by $\varepsilon(\vec{r})$. If the spatial dependence of the dielectric constant of any medium is known, the solutions to equation (2.5) will provide the solutions to the optical modes. However, the complex geometry of photonic crystals makes the solution of this equation non-trivial and, outside of the simplest cases, requires a fair amount of computational work to provide answers. The left side of equation (2.5) can be formulated as an operator Θ acting on $\vec{H}(\vec{r})$ so that it takes explicitly the form of an eigenvalue problem,

$$\Theta\vec{H}(\vec{r}) = \omega^2\mu_0\vec{H}(\vec{r}) \quad (2.6)$$

$$\Theta = \nabla \times (\frac{1}{\varepsilon(\vec{r})}\nabla \times)$$

Similarly to equation (2.5), a master equation for $\vec{E}$ could also be formulated, however it is more convenient to express the problem in terms of $\vec{H}(\vec{r})$. This is because the operator Θ is Hermitian which simplifies the computational problem [32]. After obtaining the modes $\vec{H}(\vec{r})$ for a given frequency, the following relation can be used to obtain the electric field distribution,

$$\vec{E}(\vec{r}) = (\frac{-i}{\omega\varepsilon(\vec{r})})\nabla \times \vec{H}(\vec{r}) \quad (2.7)$$

In optical fibers, the translational invariance of the refractive index profile along the z-direction leads to the following form of solutions for equation (2.5)

$$\vec{H}(x, y, z) = \vec{H}(x, y)e^{-i\beta z} \quad (2.8)$$

Where, β is the propagation constant along z (the fiber axis). The harmonic mode $\vec{H}$(x,y) is the eigenvector associated to the eigenvalue β. In the case of a wave propagating in a

homogeneous medium ($\varepsilon(\vec{r}) = \varepsilon$) equation (2.5) reduces to the Heltmholtz equation, which can be solved in a closed form. In the same manner, if the geometry of the system is simple enough to apply analytical boundary conditions at the interfaces, the electromagnetic problem can also have an analytical solution. This is the case of conventional step-index fibers. However, in the case of photonic crystal fibers the eigenvalue problem is more complicated due to the fibers complex geometry and analytical solutions are usually impossible to obtain. Powerful numerical methods are used to obtain the eigenvectors and eigenvalues of the electromagnetic problem. Nevertheless, when analyzing infinite structures, the periodic nature of a photonic crystal allows the simplification of the electromagnetic problem to a small region of the photonic crystal.

Photonic crystals can be described in terms of a periodic array of points in space called a lattice, and a unit cell which is repeated identically at every point of the lattice. The unit cell is defined as the smallest area, which by mere translations can fully represent the structure. Every point of the lattice can be defined in terms of the lattice vectors ($\overrightarrow{u_1}, \overrightarrow{u_2}, \overrightarrow{u_3}$), which are the smallest vectors that can connect one lattice point with another. All crystals have an associated lattice in Fourier space called reciprocal lattice which consists of the set of all the allowed terms in the Fourier expansion of the periodic structure. This lattice is defined in terms of the primitive reciprocal lattice vectors ($\overrightarrow{g_1}, \overrightarrow{g_2}, \overrightarrow{g_3}$) [27, 32-33].

To examine the way a photonic crystal affects the propagation of light passing through it, the dielectric constant of the structure must be expressed in terms of the lattice vector $\vec{R}$. The periodic dielectric function of a photonic crystal satisfies ε ($\vec{r}$) = ε ($\vec{r}$+$\vec{R}$). According to Bloch's theorem, the solutions of the magnetic field can be expressed as Bloch's states consisting of a plane wave modulated by a periodic function with the same periodicity as the photonic crystal,

$$\overrightarrow{H_k}(\vec{r}) = \overrightarrow{U_k}(\vec{r})e^{i\vec{k}\vec{r}} \tag{2.9}$$

where $\overrightarrow{k}$ is the wave vector, $\vec{r}$ denotes the position vector and $\overrightarrow{U_k}(\vec{r})$has the same periodicity as the lattice, i.e. $\overrightarrow{U_k}(\vec{r}) = \overrightarrow{U_k}(\vec{r} + \vec{R})$.Therefore, knowing the values of the magnetic field $\overrightarrow{H_k}$ in a unit cell, the magnetic field in all the structure can be inferred from equation 2.9. In other words, the electromagnetic problem in an infinite photonic crystal is reduced to finding the

values of the magnetic field (2.5) in a small area. In the same way, in the reciprocal lattice, a Bloch state for a wave vector $\vec{k}$ is equal to the Bloch state $\vec{k} + \vec{G}$, where $\vec{G}$ any vector of the reciprocal lattice is. This gives rise to a periodicity of the dispersion curve in the reciprocal space (or $\vec{k}$-space), expressed as $\omega(\vec{k}) = \omega(\vec{k} + \vec{G})$. Consequently, the dispersion information of the modes is contained in a region of the reciprocal space called the Brillouin zone and only wave vectors $\vec{k}$ lying inside the Brillouin zone identify an independent mode. Therefore the dispersion curves of a photonic crystal are normally presented as plots of frequency versus wave vectors in the Brillouin zone. In the following section an intuitive approach to understanding the optical properties of photonic crystals is discussed.

2.1.2 One Dimensional Photonic Crystals

A schematic illustration of a 1-dimensional photonic crystal is shown in Fig. 2.1(a), the system is a periodic arrangement of layers of two different dielectric materials. The system is repeated in the z-direction with period Λ which is of the order of the wavelength of light. A plane wave traveling along the line of periodicity will be scattered at the crystal interfaces every distance Λ. This will give rise to forward and backward propagating waves which will interfere to form standing waves within the structure. The system can also be viewed in the k-space as a line of scattering points with separation equal to the reciprocal lattice vector G = $2\pi/\lambda$. This implies that a mode with wave vector k_0 has the same dispersion and, thus, couples with a mode with wave vector $k_0 \pm$ nG, forming a new state which is strongly linked to the structure.

The dispersion of light propagating in an isotropic medium is given by:

$$\omega(k) = \frac{ck}{\sqrt{\epsilon_d}} = \frac{ck}{\eta} \tag{2.10}$$

Where, c is the speed of light in vacuum, $\epsilon_d = \varepsilon_d/\varepsilon_0$ is the medium's relative dielectric permittivity, and η is its refractive index. This dispersion relation indicates that the energy of light changes linearly with the momentum (k) and zero energy corresponds to zero momentum. Now allow a plane wave to propagate in a 1D photonic crystals in the z-direction, crossing the layers of dielectric at normal incidence, see Fig. 2.1(a). In this case, $kxy = 0$ and therefore, only the wave vector in the propagation direction (kz) will determine the dispersion properties. Due to the periodicity in the k space the point $kz = 0$

can be defined at all the scattering points ($kz = \pm nG$). This allows repeating the dispersion relation given by equation (2.10) at all the scattering points $kz = \pm nG$, blue lines in Fig. 2.1(b).

As it is shown in Fig. 2.1(b), when the first band $\omega = \pm ck/n$ (red lines), reaches the edges of the Brillouin zone it is translated back into the zone and is named as second $\omega = c/n(k0 + G)$ and $\omega = -c/n(k0 - G)$. This shows that the optical modes fold back on themselves as they reach the Brillouin zone. This folding arises from the scattering of neighboring sites $kz = \pm G$ and leads to very different optical properties for a periodic material compared to an isotropic medium.

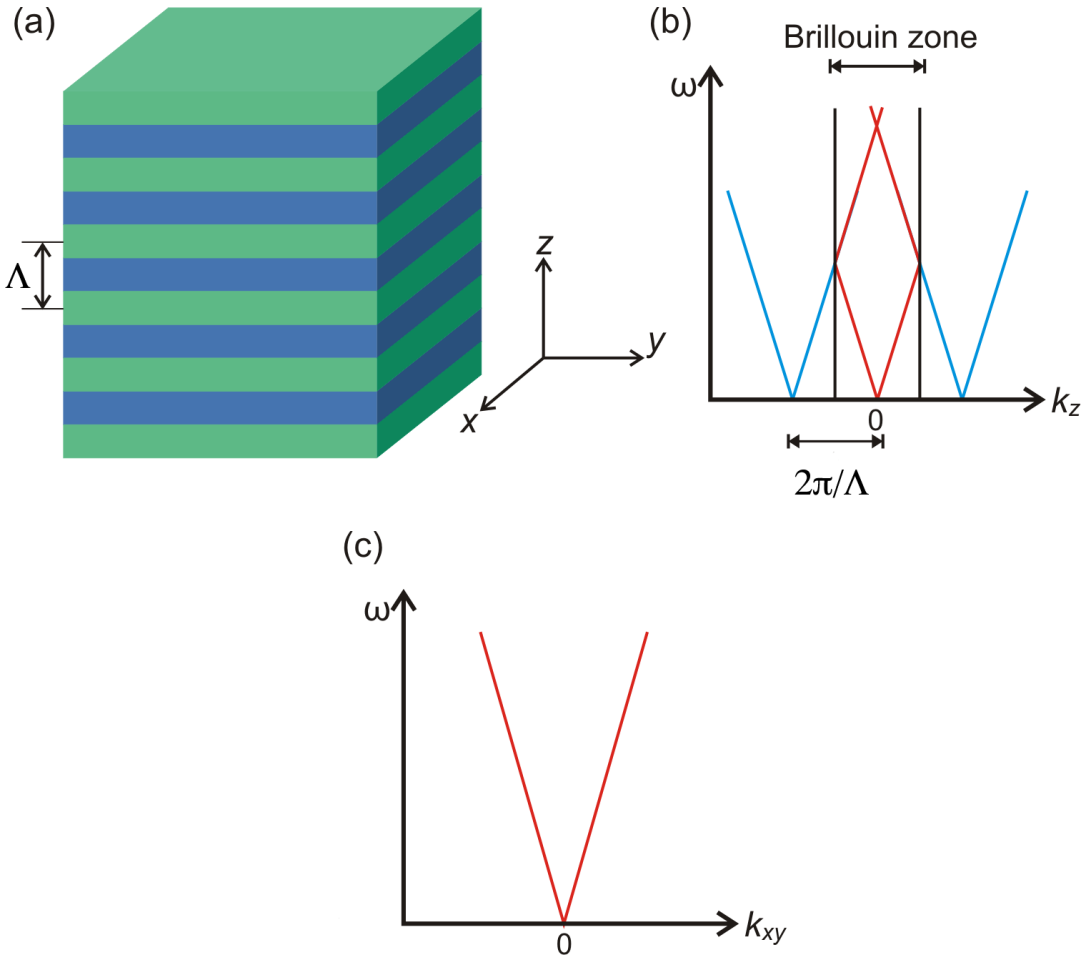

Fig. 2.1: (a) Illustration of a 1-dimensional photonic crystal with period Λ and reciprocal lattice vector G. Schematic plots of the dispersion relations of plane waves propagating in the photonic crystal in the z-direction and on the xy plane, (b) and (c) respectively.

Fig. 2.1(c) shows the dispersion relations of a wave propagating in the xy-plane, in this case the dispersion is simply that of light propagating in a isotropic medium. The schematic shown in Fig. 2.1(b) considers the weak scattering approximation, a condition that assumes no interaction between the dispersion bands from different lattice sites. The weak scattering approximation is limited to structures where the difference in the dielectric constant between the layers is small. When the refractive index difference is large the weak scattering approximation is not valid and one must solve equation (2.6) to obtain the optical modes in the structure.

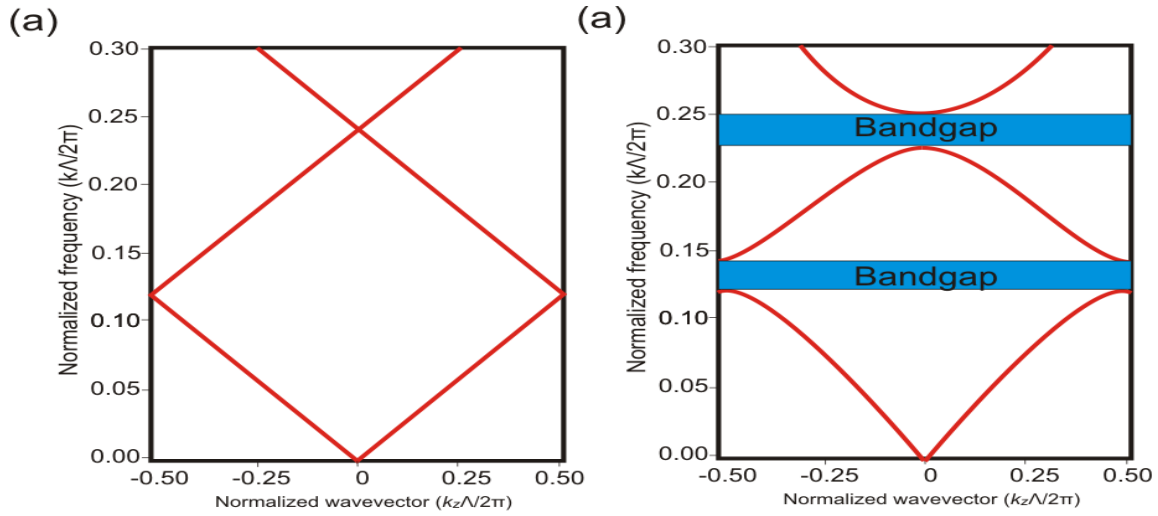

Fig. 2.2: Dispersion relation of light propagating along a periodic dielectric structure, with dielectric contrast difference between the layers of zero and three for (a) and (b) respectively.

The dispersion relations of two different 1D photonic crystals calculated by solving equation (2.6) are shown in Fig. 2.2. When light propagates in a structure where both dielectric regions have the same refractive index n (a single slab of material) its dispersion curve is just the dielectric line given by equation (2.10), see Fig. 2.2(a). Conversely, Fig. 2.2(b) plots the dispersion of light propagating through a 1D photonic crystal where the dielectric layers have a difference in dielectric constant of 3. The blue shaded areas show that there are frequency regions where optical modes do not exist at all. These regions are calling photonic band gaps. For a physical description of the band gap formation it is useful to consider the electric field distribution directly above and below the first gap, which as seen in Fig. 2.2(b) occurs at the edge of the Brillouin zone, at $k = \pi/\Lambda$. At this position, the optical modes correspond to standing waves with wavelengths equal to twice the crystal lattice constant 2Λ. There are

only two electric field distributions (for the first two bands), that form standing waves and satisfies the boundary conditions and the symmetry of the system. For the first solution the maximum intensity is located at high refractive index layers while the second one is concentrates in the low dielectric constant layers, (see Fig. 2.3). Therefore, it becomes clear that these two modes have different effective mode indices. The dispersion curve also shows that both modes have the same wave vector ($k = \pi/\Lambda$) and hence the same wavelength. However, the mode concentrated in the high refractive index material experiences a greater effective index and, thus, a lower frequency than the mode concentrated in the low refractive index material. This difference in frequency provides the energy gap between the high and low index bands in the photonic crystal, analogous to the valence and conduction band in a semiconductor. It is important to note that band gaps always appear in one dimensional photonic crystal for any dielectric constant difference. And as the refractive index contrast increases the band gap widens.

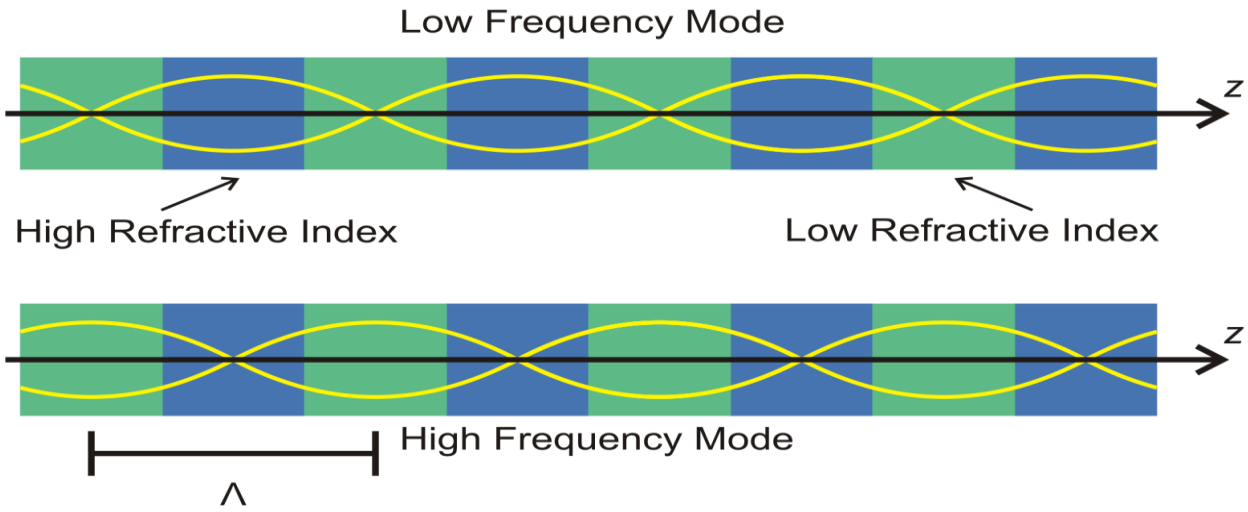

Fig. 2.3: Distribution of the electric field in a one-dimensional photonic crystal. For both modes k trans = 0 however, the mode localized in the high refractive index regions has a lower frequency than the mode which concentrated in the low refractive index regions.

One dimensional photonic crystals are widely used in many optical devices where the transmission of light for certain frequencies needs to be suppressed, light within this range will be reflected very efficiently. Examples of 1D photonic crystals are fiber Bragg gratings,

widely used in optical telecommunication systems, Bragg filters for diode lasers, antireflection coatings, etc.

2.1.3 Two Dimensional Photonic Crystals

Two dimensional photonic crystals have a periodic pattern in the xy-plane while remain constant in the z-direction. These structures can be designed to have a photonic band gap for light propagating in the structured plane. In a similar way to the one-dimensional case, to qualitatively understand the dispersion properties of two-dimensional photonic crystals one can use the weak-scattering approximation. For the specific type of photonic crystals of interest in this thesis, photonic crystal fibers, the structure can be represented as a closed packed array of scattering sites (holes) arranged in a triangular lattice, see Fig. 2.4(a). In this case the primary lattice vectors are equal in length at a 60° angle to each other, and can be chosen as follows:

$$\overrightarrow{R_1} = \frac{\Lambda}{2}(\vec{x} + \vec{y}\sqrt{3}) \tag{2.11}$$

$$\overrightarrow{R_2} = \frac{\Lambda}{2}\left(\vec{x} - \vec{y}\sqrt{3}\right) \tag{2.12}$$

The scattered light off the surface may be obtained by taking the Fourier transform of the lattice and the first set of scattered modes corresponds to those of one lattice vector, of which there are six solutions. By taking the Fourier transform of the crystal it is found that the lattice in k space also forms a triangular lattice rotated 30° with respect to the real-space lattice, as depicted in Fig. 2.4(b).

The reciprocal lattice vectors $\overrightarrow{G1}$ and $\overrightarrow{G2}$ are related to the real space lattice vectors by

$$\overrightarrow{R_\iota}.\overrightarrow{G_J} = 2\pi.\delta_{ij},\ i,j = 1,2, \tag{2.13}$$

Where, δij is the Dirac delta function. The reciprocal lattice vectors can be written as follows:

$$\overrightarrow{G_1} = \frac{2\pi}{\Lambda}\left(\vec{x} + \vec{y}\frac{\sqrt{3}}{3}\right) \tag{2.14}$$

$$\overrightarrow{G_2} = \frac{2\pi}{\Lambda}\left(\vec{x} - \vec{y}\frac{\sqrt{3}}{3}\right) \tag{2.15}$$

The angle between the lattice vectors of the real- and k-space is also 30°. The irreducible Brillouin zone corresponding to a six-fold symmetric unit cell is illustrated as the black area

in Fig. 2.4(b). The high symmetry points of the reciprocal lattice are labeled Γ, M, and K. As in the 1D case, the dispersion relation of a 2D photonic crystal can be obtained by drawing the dispersion of light from each scattering point (weak scattering approximation). However, in this case the visualization is more complicated than in the 1D case and thus not very practical. For the purposes of this chapter it is more convenient to obtain the dispersion relations by solving the master equation.

As photonic crystal fibers are invariant along the fiber axis (z), from equation (2.8) the optical modes can be written as:

$$\vec{H}(\vec{r}) = \vec{H}(\overrightarrow{r_t})e^{-i\beta z} \tag{2.16}$$

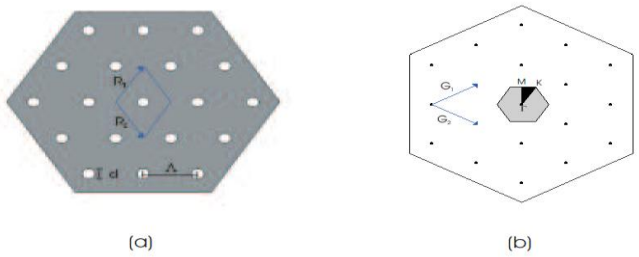

Fig. 2.4: (a) Triangular lattice of circular holes, real space primitive vectors $\overrightarrow{R_1}$ and $\overrightarrow{R_2}$. The area inside the blue lines is the unit cell. (b) The crystal can be represented in the k-space as a triangular lattice of scattering points with corresponding reciprocal lattice vectors $\overrightarrow{G_1}$ and $\overrightarrow{G_2}$. The shaded hexagon is the Brillouin zone, the irreducible Brillouin zone is the darker area. The marked points in the Brillouin zone are conventionally known as Γ, M and K.

Where, $\overrightarrow{r_t}$ is the transverse component of the position vector $\vec{r}$, $\beta = k_z$ is the propagation constant (axial component of the wavevector). β is conserved across every region of the structure. The optical modes $[\vec{H}(\overrightarrow{r_t})]$ of the structure can be calculated to obtain the band structure of a 2D photonic crystal. From Bloch's theorem and due to the symmetry of the triangular lattice, the band structure is shown for the irreducible Brillouin zone. Fig. 2.5 shows the band diagrams of a triangular photonic crystal calculated by scanning the transverse component of the wave vector $\overrightarrow{K_t}\Lambda$ at 16 points along the boundaries of the irreducible Brillouin zone (see Fig. 2.4) for βΛ = 20 left and $\beta\Lambda$ = 21 right. In both cases a photonic band gap appears.

As $\beta\Lambda$ is increased the bandgap is pushed towards higher frequencies whilst. The different bands, as in the one dimensional case, represent optical modes localized mainly in the silica

and air regions, high and low refractive index. However, the mode field distribution is now in two-dimensions and its structure is more complicated than in the 1D case.

An important feature of this gap map is that some of the band gaps cross the air line, which is the region of the map with $\beta < k$. Indicating that electromagnetic waves with frequencies within these gaps are free to propagate in air. Therefore, light propagating in a region of air surrounded by the photonic crystal is not allowed to leave the air region but will be evanescent in the photonic crystal cladding due to interference effects. The presence of these band gaps in the cladding structure opens the possibility of light guidance in an air core. It is important to notice that the PBGs overlap the air line only at some narrow regions. Therefore light can be guided in air only over narrow spectral intervals. A key point of the gap map (for air-silica) is that no gap extends for all values of $\beta\Lambda$ indicating that a complete 3D bandgap gap does not exist in a 2D photonic crystal.However a 2D bandgap is enough for band gap guidance in the transverse direction [10].

In the case that the core is formed by a medium that has higher refractive index than the photonic crystal cladding, i.e. the blue region of Fig. 2.5, light is free to propagate in the higher index core but will be evanescent in the lower index cladding. Therefore, the PCF operates in a similar way as a conventional fiber, for certain incidence angles light will be total internal reflected in the core-cladding interface.

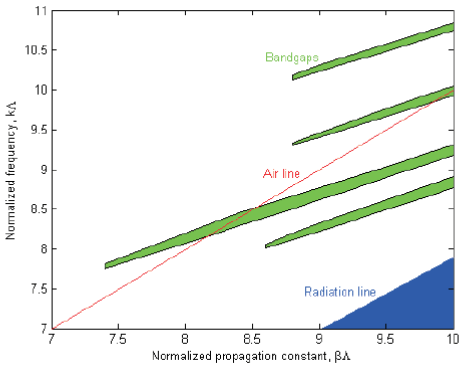

Fig. 2.5: Band map for a triangular lattice of circular holes in silica with f = 45% The blue region is where holey fibers work, in this region light is transmitted by modified total internal reflection. Inside the band gaps, green regions, light could be guided by the PBG effect. The regions of the band gaps with $\beta < k$ may be used to guide light in an air core.

2.2 Fabrication of PCFs

Optical fiber fabrication typically involves two stages, preform fabrication and fiber drawing. A preform is a large-scale replica of the fiber normally ~ 50 cm in length and ~ 20mm in diameter (for PCFs). A preform is drawn down to micro-scale dimensions on a fiber drawing tower (see Fig. 2.6). During the relatively short history of PCFs they are now made in many laboratories around the world using various preform synthesis methods, such as: stacking of capillaries and rods, sol-gel casting [34], ultrasonic drilling [35], extrusion from bulk glass with low softening temperature [36] and rolling flexible material sheets into tubes [37], each of which has advantages and disadvantages depending on the glass used and the desired fiber geometry.

For silica PCFs, capillary stacking has become the most widely used technique mainly due to the design flexibility it offers. In this approach, firstly, approximately half a meter long capillaries with a typical outer diameter of ~ 1mm are drawn from a starting tube of high-purity synthetic silica with an outer diameter of 10 − 20mm. The inner/outer diameter of the starting tube determines the ratio between the hole diameter and the lattice pitch (d/Λ) in the drawn fiber. The capillaries are stacked on a horizontal rig in a close-packed arrangement which reproduces the structure that is to be obtained in the final fiber. These packages are then inserted into a jacket tube and packing silica rods of different diameters are carefully inserted to ensure mechanical stability of the structure. A rod placed in the centre of the stack acts as the solid core of index-guiding PCFs and a tube is inserted if a hollow-core PBGF is to be obtained. The resulting PCF preform is then drawn down to canes of few millimeters diameter. The top end of the capillaries can be sealed in order to create pressure gradient to balance the collapsing effect of surface tension during drawing. Vacuum is normally used during this step to prevent the capillaries from moving. The resulting cane is inserted into a solid jacket tube and by applying a second drawing stage a PCF is produced. In this latest stage, the use of vacuum, pressure and the control of the drawing parameters (tension, furnace temperature, feed speed, fiber speed, etc.) are very important to obtain a fiber with optimal characteristics. Fig. 2.7 shows a summary of the stack and draw fabrication process.

An amazing property of silica-air photonic crystal fibers is that the air channels in centimeter scale preforms are preserved when drawn down to the micro-scale. After drawing, these

micrometer wide channels run along fibers that can be hundreds of meters of even a couple of kilometers long. During drawing the preform is mounted in a holding chuck attached to a feed mechanism that lowers the preform into a furnace at the feeding speed (V_p). The furnace temperature is raised above the glass-softening temperature about 1900◦ C − 2200◦ C. As the glass softens a "drop" forms due to gravity. The drawn fiber is taken up by the capstan which controls the draw speed (V_f). A variety of furnaces can be used to heat the preform. As turbulence around the fiber causes unacceptable variations in the fiber diameter, the furnace must provide laminar gas flow and must also give off no particles that might attach to the preform and degrade the fiber strength. The most common furnaces used that meet these requirements are graphite resistance and induction furnaces. The advantage of the induction furnace is its compact size compared to resistance furnaces. The furnace includes inert gas inlets to provide laminar flow of a sufficient quantity to maximize fiber strength and minimize diameter variations characteristic of turbulent gas flows. Furnace temperature is measured with an optical pyrometer from either the outer surface of the heating element or directly from the preform neck-down depending on the furnace set-up, the former being the more typical configuration. The temperature can be controlled to within 1◦C.In order to maintain a uniform fiber diameter; the drawing process includes a diameter control loop. The fiber diameter is monitored as it exits the furnace. The output signal from the diameter monitor is used to automatically adjust the speed of the drawing capstan using a PID controller to obtain a constant diameter. Before the fiber reaches the capstan it is coated with a protective polymer. Coating is required to protect the pristine silica surface from scratches and abrasion and it preserves the intrinsic strength of silica. The coating usually consists of two layers of acryl ate, a softer inner layer and a harder outer layer. However, it is possible to use the second coating only. Acryl ate coating is applied in liquid phase and is solidified by UV-curing. Before coating the fiber must be cooled below 80◦ C. Thus, between the furnace and the coating cup the fiber is cooled down by the surrounding air. At high drawing speeds and with limited tower height it may be necessary to use forced cooling using inert gases as helium. After coating the fiber passes over a capstan onto a fiber take-up that winds the fiber onto a spool. Prior to coating, the fiber surface is exposed to potential ambient contamination that will reduce the fiber strength. The fiber is therefore drawn in a clean room.

2.3 Guidance mechanisms in photonic crystal fibers

The "simplest" optical fiber has a step-index geometry which consists of a central doped silica cylinder with refractive index η_{co} surrounded by a silica cladding whose refractive index η_{cl} is slightly lower than that of the core, Fig. 2.7(a). The refractive index profile of optical fibers is constant along the fiber axis z. As the system is invariant under any translation along the z-axis, electromagnetic waves propagating along this axis have a dependence of $exp(i\beta z)$ along the propagation direction. The propagation constant of the wave is β [equation (2.8)] which is the

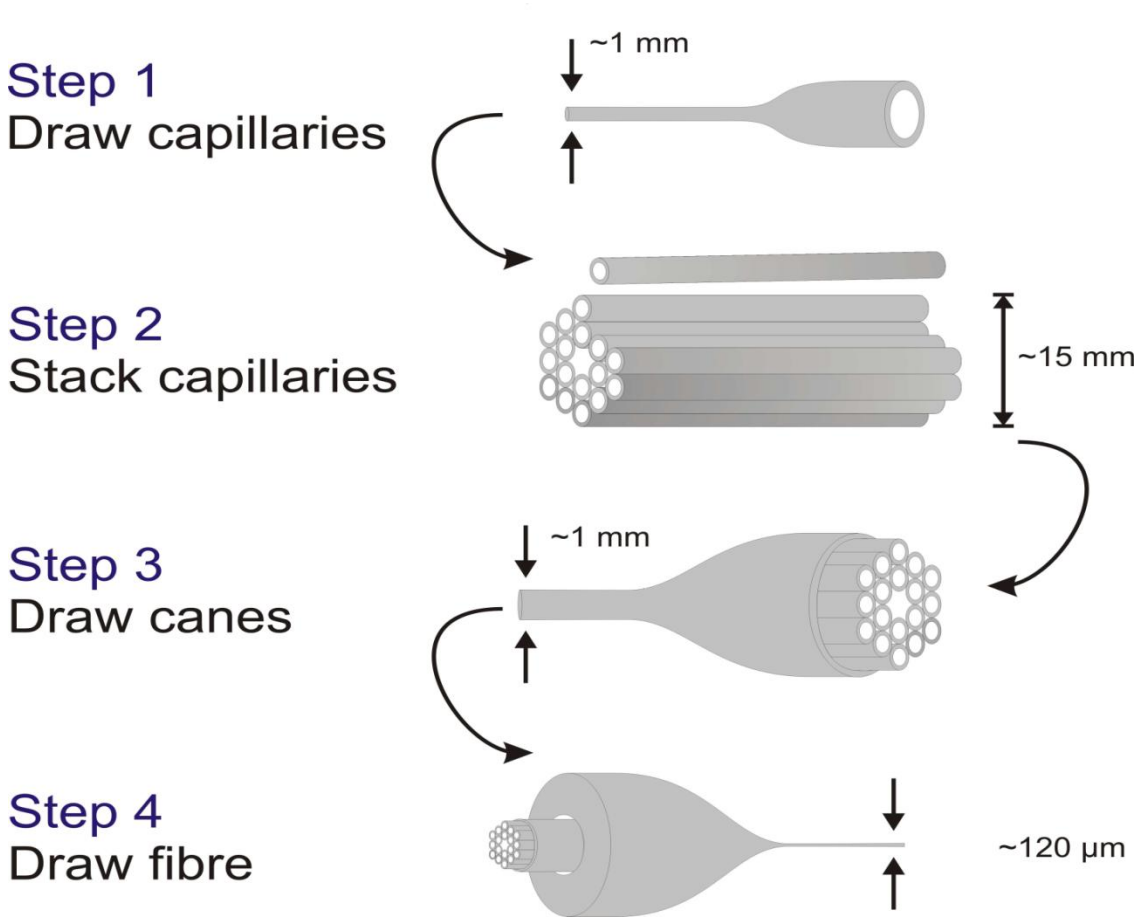

Fig. 2.6: Summary of the stack and draw PCF fabrication process. Silica capillaries and rods drawn and stacked in order to create a fiber preform. The preform is drawn down to a cane of ~1mm and finally this cane is introduced in a jacket tube and drawn down to a fiber.

component of the wave vector. The propagation constant of light traveling in a medium with refractive index η is either equal to or smaller than the absolute value of the wave vector, i.e.

$\beta \leq \eta\overrightarrow{k_0}$. Therefore, β must be less than or equal to $\eta_{co}k_0$ to propagate in the core and less or equal to $\eta_{cl}k_0$ to propagate in the cladding. The enclosed geometry of optical fibers defines resonant conditions on β which forces all the possible solutions of the Maxwell equations and the values of β to be discrete. Each allowed field distribution (mode) in the fiber corresponds to an allowed β. Modes for which $\eta_{cl}k_0 \leq \beta \leq \eta_{co}$ are called guided modes or core modes, as they are propagative in the core and evanescent in the cladding. On the other hand, modes with $\beta \leq k_0\eta_{cl}$ are called cladding modes. These modes are not evanescent in the cladding. Guided modes usually have low loss whereas cladding modes usually experience high loss. It is convenient to define the effective mode index of a mode as$\eta_{mode} = \beta/k_0$.

Since the size of the cladding is usually much bigger than the core size, the propagation constant of the cladding modes can be considered as continuous and to form a band. A core mode will inevitably couple into cladding modes if its propagation constant falls within a band of cladding modes. Therefore, in order to design optical fibers able to guide light, the propagation constant of the desired core modes must be outside the bands of cladding modes -this statement is not strictly valid for a certain type of PCFs.

As it has been previously described, there are two possible methods of making such an optical fiber (see Fig. 2.8). Firstly, index-guiding fibers, in which the core index is higher than the largest possible effective mode index of any cladding mode as illustrated in Fig. 2.8(a). This is normally done either by doping the core glass so as to increase its refractive index compared to the lower-index glass which forms the cladding or by structuring the cladding so as to decrease its refractive index compared to the core index, Fig. 2.7. Both, conventional fibers and index-guiding PCFs fall into this category. Secondly, photonic band gap fibers, in which a 2-dimensional photonic band gap formed by a periodic cladding divides the continuum of cladding modes into different bands.

2.3.1 Index-guiding PCFs

In conventional optical fibers, light propagation is due to total internal reflection at the core-cladding interface. In these fibers, the maximum cladding mode index is limited by the cladding refractive index, which must be lower than the core refractive index. Under this

condition, there can exist a core mode whose mode index is bigger than the material index of the cladding -see Fig. 2.8(a). Index guiding PCFs guide light by means of a modified total internal reflection mechanism, in which light propagates in a solid core, surrounded by a structured cladding (not necessarily periodic). In these fibers, the maximum cladding effective mode index is reduced not

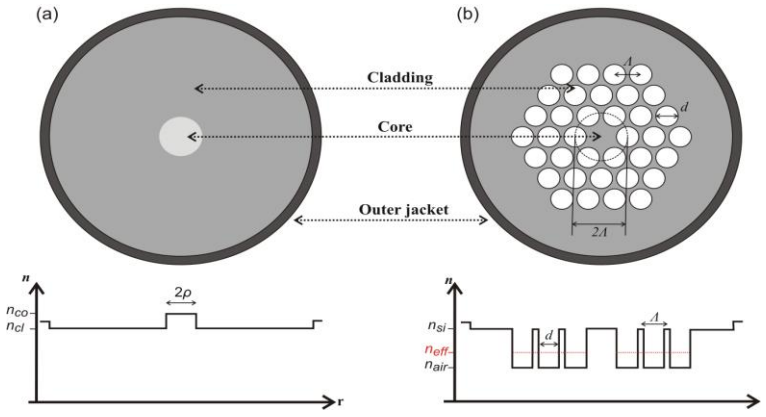

Fig. 2.7: Cross sectional area and refractive index profile of (a) a conventional step-index optical fiber and (b) solid core PCF. In (b) the white and grey regions are air and silica respectively. The photonic crystal cladding is an ideal hexagonal lattice with parameters: pitch Λ and hole diameter d.

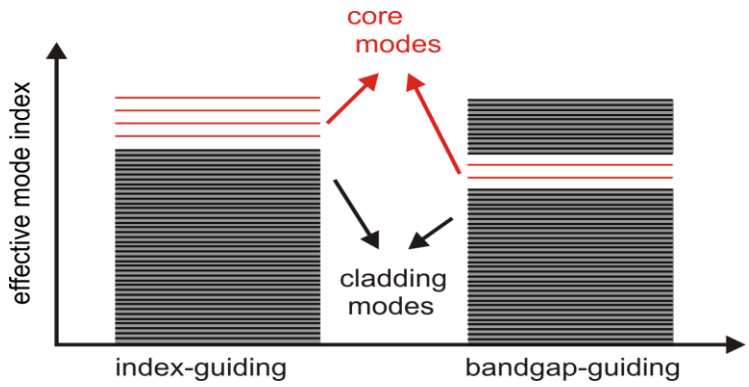

Fig. 2.8: Schematic illustration of the two possible guidance mechanisms of optical fibers. Cladding modes are represented with black lines and red lines are the discrete guided modes. In index guiding fibers the core refractive index is greater than the cladding refractive index (left). In band gap fibers the continuous of allowed cladding modes is split in two bands. The core modes are located between these two cladding bands (right).

by using different materials but by having micro-holes in the cladding. The low cladding mode index is somewhere between the bulk material index and that of air. This ensures the core modes to have greater mode refractive index than the cladding modes. Thus, light

incident at certain angles propagates in the high refractive index core by a form of total internal reflection as in conventional optical fibers [12]. Fig. 2.8 depicts a comparison of a typical refractive index profile of a conventional step-index fiber and an index-guiding PCF.

Some of the basic optical properties of index guiding PCFs can be related to fundamental concepts concerning conventional optical fibers. For this, Birks et al.[13] proposed the now well known effective index method. This method consists of interpreting the structured cladding as a solid medium with a properly chosen effective refractive index, η_{eff}. The effective index method uses a scalar model to evaluate the periodic structure of the cladding in order to calculate η_{eff} . The first step of the effective index method is to determine the fundamental mode or fundamental space-filling mode of the photonic crystal cladding (the cladding mode with the highest refractive mode index). This is done by solving the wave equation (Eq. 2.5) within a cell centered at one of the holes in the periodical lattice. The propagation constant of the resulting fundamental space filling mode (β_{FSM}) is the maximum propagation constant allowed in the cladding, and can be used to define the effective index $\eta_{eff} = \beta_{FSM}/k_0$. The red line in Fig. 2.9b indicates the effective refractive index of the cladding. The resulting waveguide consists of a solid core and a solid cladding with refractive indices η_{co} and η_{eff} respectively. As a result, some modelling elements for standard optical fibers can be applied for PCFs.

Similarly to conventional fibers, the propagation constant of any mode supported in the core needs to be$k_{co} > \beta > \beta_{FSM}$. The effective index method which is valid for small holes provides a good qualitative description of the optical properties of index-guiding PCF [38].

2.3.2 Properties of Index-guiding PCFs

The number of guided modes supported by step-index fibers depends on the normalized frequency:

$$V = k_0 \rho \sqrt{(\eta_{co}{}^2 - \eta_{cl}{}^2)} \tag{2.17}$$

Where, ρ is the core radius, η_{co} and η_{cl} are the refractive index of the core and cladding respectively [39, 8]. The smaller this parameter the fewer guided modes supported by the core. If at a given wavelength $V < 2.405$, the fiber can only guide one pair of orthogonally polarized modes which have the same β, and the fiber is said to be single-mode. Either of

these two degenerated modes is known as the fundamental mode. The design of single mode fibers requires a combination of small core size to wavelength ratio, typically core sizes between 8.3 to 10 μm for 1550 nm operation, and a small difference in refractive index between the core and cladding. Equation (2.17) indicates that step-index fibers are always multi mode for sufficiently small wavelengths.

The normalized frequency of PCFs is defined as an effective value

$$V_{eff}(\lambda) = k_0 2\Lambda \sqrt{\left(\eta_{silica}{}^2 - \eta_{eff}{}^2\right)} \tag{2.18}$$

Where, 2Λ is the core diameter. Endlessly single mode behaviour in PCFs at any wavelength from the UV to the near infrared was observed by Birks et al. [13]. Fibers with $d/\Lambda \leq 0.4$ do not support higher order modes as their normalized frequency remains smaller than 2.405 for any wavelength [18]. Endlessly single-mode guidance in PCF originates from the strong wavelength dependence of the cladding refractive index. Light of long wavelengths penetrates into the cladding region and thus, part of its energy is concentrated in the air regions, whereas, shorter wavelengths concentrate most of the energy in the silica core, forcing the core/cladding index difference to fall as the wavelength gets shorter. This counteracts the usual trend towards multimode behavior and $V_{eff}(\lambda)$ is almost kept constant. As single mode operation does not depend upon the core size but only on the air filling fraction [18], single mode fibers with large cores can be developed, for example a single-mode PCF at 458 nm with core diameter of 22 μm was fabricated [40]. A conventional fiber would require a core $\sim$ 10 fold smaller to be single-mode at this wavelength. Large mode area single mode PCFs are able to transmit higher power before nonlinear effects affect the beam quality. Such fibers are desirable in laser and amplifiers [41-42].

The optical properties of index-guiding PCF are extremely sensitive to the cladding and core structure. By choosing the pitch, hole and core size, these fibers can present many interesting dispersion, modal and nonlinear properties which are impossible to obtain with standard step-index fibers. For example, PCFs can exhibit unique dispersion properties [21, 23], like flat dispersion covering a broad window [22, 43] and the zero dispersion wavelength can be engineered to be below 1.28 μm which is the ZDW (zero dispersion wavelength) of conventional single-mode fibers [19]. High nonlinearity is another interesting property of

index guiding PCFs. Fibers with high air filling fraction can tightly confine light in a small core and thus have high nonlinearity due to small mode area. Nonlinearities 10-50 times greater than that of conventional fibers can easily be achieved with PCF technology. Many nonlinear optical processes such as wavelength conversion, Raman amplification [44], optical switching [45, 46], parametric processes [47], soliton squeezing [48-49], and super continuum generation [17, 50-53] have been observed in these fibers.

2.4 Classification of photonic crystal fiber

2.4.1 Solid core photonic crystal fiber

The first fiber with a photonic crystal structure was reported by Russell and his colleagues in 1996. Even if it was a very interesting research development, the first PCF did not have a hollow core as shown in Fig. 2.9 and consequently it did not rely on a photonic band gap for optical confinement. In fact, in 1996 Russell's group could produce fiber with the necessary air-hole triangular lattice but the air-holes were too small to achieve a large air-filling fraction which is fundamental to realize a PBG. Measurements have shown that this solid-core fiber formed a single-mode waveguide that is only the fundamental mode was transmitted over a wide wavelength range. Moreover the first PCF had very low intrinsic losses due to the absence of doping elements in the core and a silica core with an area about ten times larger than that of a conventional single mode fiber (SMF), thus permitting a corresponding increase in optical power levels.

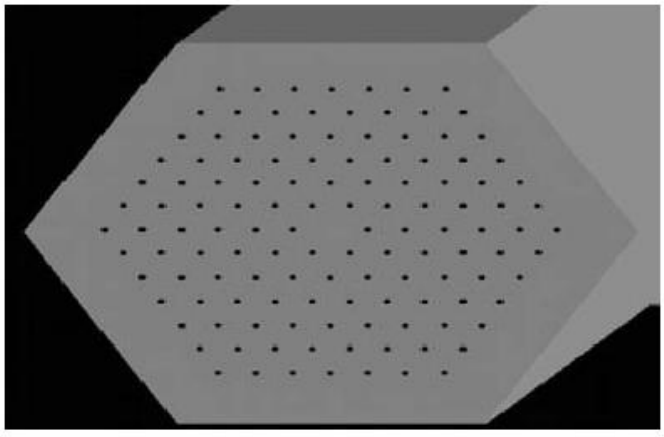

Fig. 2.9 **:** Schematic of the cross-section of the first solid-core photonic crystal fiber with air hole diameter of 300 nm and hole-to-hole spacing of 2.3 μm [32].

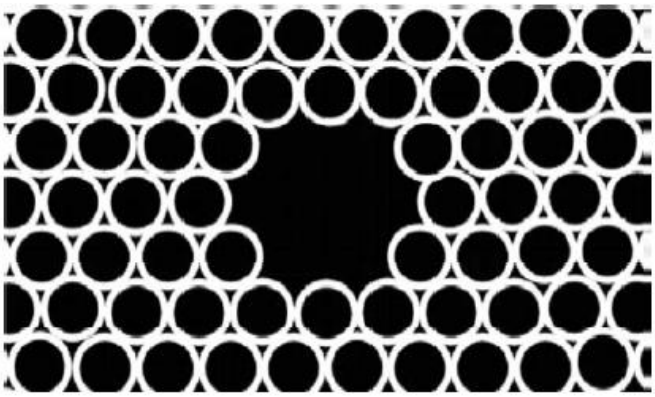

Fig. 2.10: Schematic of the cross-section of the first hollow-core PCF, with hole-to hole spacing of 4.9 μm and core diameter of 14.8 μm [32].

2.4.2 Hollow core photonic crystal fiber

After moving his research group to the University of Bath where PCF fabrication techniques were steadily refined, Russell and his co-workers were able to report the first single mode hollow-core fiber in which confinement was due by a full two-dimensional PBG as reported in Fig. 2.10. They realized that the photonic band gap guiding mechanism is very robust since light remains well confined in the hollow core even if tight bends are formed in the fiber. Initial production techniques were directed simply at the task of making relatively short lengths of fiber in order to do the basic science but many research teams are now working hard to optimize their PCF production techniques in order to increase the lengths and to reduce the losses.

2.5 Modelling Photonic Crystal Fiber

In the last years, various methods have been developed for the analysis of photonic crystal fibers. Although some the fundamental concepts used in conventional fibers modeling can still be used, the complex structure of the photonic crystal cladding requires the employment of full vectorial methods. Specially, photonic band gap guiding fibers have been analyzed by novel methods which are related to the methods used for the calculation of band gaps in semiconductors [32]. A brief description of the numerical methods used in this thesis to calculate the optical properties of hollow-core PBGF is presented in the following sections. A detailed description of the most widely used numerical methods for the analysis of photonic crystal fibers can be found in [54, 55].

2.5.1 Full vectorial plane wave expansion method

The plane wave method was the first accurate method for the calculation of band maps in photonic crystals [56]. Prove of this is that the first structure that had a photonic bandgap was found using this method [57], and now it is one of the most applied tools in the analysis of photonic band gap fibers. To understand this method recall that in Fourier space the reciprocal lattice vectors form a complete orthogonal set and thus any function can be expanded as a linear superposition of them [58-61]. In this way the optical modes $[\vec{H}_{\vec{k}}(\vec{r})]$ can be expressed as follows:

$$\vec{H}_{\vec{k}}(\vec{r}) = \sum_{\vec{G}} \sum_{\gamma=1,2} \vec{h}_{\vec{K}+\vec{G},\gamma}\, e^{j(\vec{k}+\vec{G}).\vec{r}} = \sum_{\vec{G}} \vec{H}_{\vec{k}}\,(\vec{G}) e^{j(\vec{k}+\vec{G}).\vec{r}} \qquad (2.19)$$

Where the basic functions are $e^{\vec{G}.\vec{r}}$, with $\vec{G}$ being a vector of the reciprocal lattice, $\vec{k}$ is the wave vector, and γ represents the two polarizations of the field orthogonal to $\vec{k}+\vec{G}$.

For the analysis of photonic band gap fibers, knowledge of a complete map of all the modes allowed in the photonic crystal cladding is indispensable. Since Plane Wave Expansion Methods assume infinitely periodic structures they are ideal for this problem. In this thesis the freely available version developed by Johnson and Joannopoulos at MIT [32] is used to calculate band gap diagrams and DOS plots. This particular implementation fixes the propagation constant β and solves for the frequency ω, therefore it is not possible to include material dispersion into the computation. An implementation of the plane wave expansion method which solves for the propagation constant for a fixed frequency has been developed by Pearce et al. [62].

To determine the existence of a photonic band gap it is in principle required to calculate the frequencies of the modes for all possible $\vec{k}$ vectors. This corresponds to all the points inside and at the boundaries of the Brillouin zone. However, symmetries give rise to a further reduction on the $\vec{k}$ vectors that need to be considered. It is widely accepted that varying the $\vec{k}$vectors along the periphery of the irreducible Brillouin zone is sufficient in order to determine the existence of a band gap.

Since plane wave expansion results in a periodic electromagnetic field, it cannot be directly applied to the study of defects such as that shown in Fig. 2.11(a). However, for this task the

plane wave methods may still be applied if an auxiliary super structure that contains the defect and several periods of the photonic crystal is considered as the unit cell [63]. The real structure that is simulated with the supercell method Fig. 2.11(b), is a periodic structure in which the defect and several periods are periodically repeated, for this reason the size of the supercell has to be large enough to guarantee that neighbor defects do not interact with each other.

A drawback of the PWEM is the high number of terms needed to accurately represent small features. This is particularly important when considering PBGF with strut thicknesses being less than one tenth of a wavelength while the core is tenths of wavelength across. For example Steel found that they needed 2^{17} terms to model a standard PCF [63]. Another draw-back of PWEMs is that they required a structured mesh therefore in order to accurately model complicated geometries a large number of terms is required. Hence, in this thesis I adopted the finite element method (FEM) described below to model the modes of HC-PBGFs.

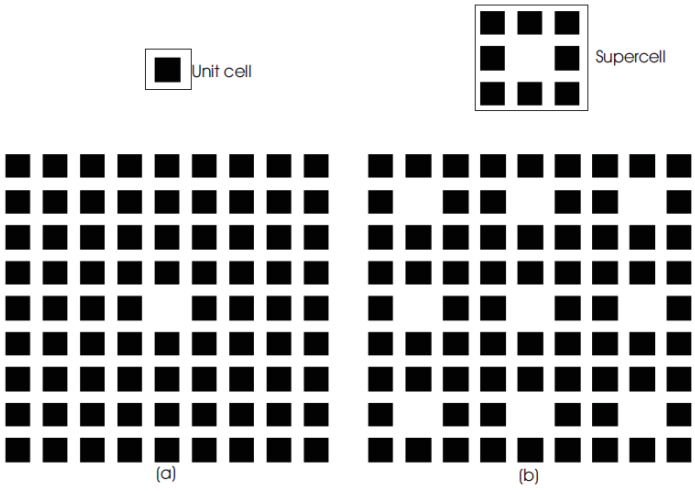

Fig. 2.11: (a) Square unit cell and structure with a central defect. (b) Illustration of a supercell of size 3x3 required in order to simulate the central defect. In the structure considered using the supercell approximation the defect is repeated periodically [62].

2.6 Loss mechanisms in photonic crystal fiber

Optical fibers are used to transport light over distances ranging from meters to thousands of kilometers. Over such distances, even small imperfections can lead to substantial effects. Conventional silica fibers have attained such an amazing degree of perfection that their losses (only about 0.2 dB/km at 1.55 μm) are limited by a combination of intrinsic material absorption and scattering from microscopic density fluctuations. At longer wavelengths, on the other hand, such as the 10.6 μm high-power lasers used for many industrial and medical applications, silica and other common fiber materials are not transparent at all.

One of the promises of hollow-core photonic-band gap fibers is that they may allow for lower losses than are possible with solid-core fibers, by relaxing the fundamental limitations imposed by solid material properties. There is a tradeoff between losses that decrease with R (losses associated with field penetration into the cladding), and losses that increase with R (losses associated with coupling between modes). This makes the choice of R a delicate balancing act that is crucial for fiber performance.

2.6.1 Cladding losses

Three important loss mechanisms are associated with the amount of field penetration into the cladding:

1. material absorption
2. radioactive leakage due to the finite crystal size
3. scattering from disorder.

All of these will tend to decrease as the core radius R increases. We will show that they typically decrease asymptotically as $1/R^3$.

Of these three loss mechanisms, the simplest one to analyze is material absorption. This can be described by a small imaginary part $i\kappa$ that is added to the real refractive index η (κ is called the extinction coefficient). Because $\kappa \ll \eta$ for transparent materials, one can obtain essentially exact results for the loss by starting with the eigenmode of the lossless structure and employing perturbation theory. Therefore, a useful dimensionless Fig. of merit for a hollow-core fiber mode is the ratio α/α_0. This is called the absorption suppression factor, the factor by which loss is decreased due to the portion of light in air [32].

What is the source of this $1/R^3$ power law? The key fact is that the contribution to the loss from a particular absorbing material is proportional to the fraction of the electric-field energy in the material. One might jump to the conclusion that, for a core-guided mode (not a surface state), the losses will scale as 1/R: if the field penetrates a certain distance dp into the cladding, then the fraction of field in the cladding goes as the penetration area $2\pi Rdp$ divided by the core area πR^2, yielding $\sim 1/R$. Such an argument, however, assumes that the field amplitude |E| in the cladding compared to the core is independent of R, and in fact this is not the case. This is easiest to see for the te01 mode, which by analogy with the metal waveguide has a node in E near r = R. As a consequence, the te01's cladding |E| is proportional not to the field at r = R (which is ≈ 0) but rather to the slope d|E|/dr at r = R, which scales as 1/R for a fixed max |E| in the core. As a result, $|E|$ in the cladding picks up an additional $1/R^2$ factor, and the absorption losses scale as $1/R^3$.

Another cladding-related loss is radioactive leakage. Because a real photonic crystal fiber cannot have an infinite number of crystal periods, the fields will have a small exponential tail beyond the edge of the crystal, which will couple to radiating modes. Again, this loss scales as $1/R^3$: 1/R from the surface area/ volume ratio, and $1/R^2$ from the field amplitude scaling in the scalar limit. As a practical matter, however, such radiation can be more easily reduced by simply increasing the number of periods. For a high-contrast band-gap fiber such as the ones discussed in this chapter, the radioactive leakage typically decreases by a factor of ten for every period or two that is added to the cladding. As a result, even the most stringent loss requirements can be met by including a few dozen periods at most.

Finally, one can also have losses from disorder, which causes light to scatter and radiate by breaking translational symmetry. Because photonic-crystal fibers typically have many high-contrast interfaces, the most serious problem seems to be due to surface roughness, especially in silica-based fibers at wavelengths where the absorption is small. A detailed analysis of disorder is complicated, but a few general statements can be made for the usual case in which the length scale of the roughness is much smaller than the wavelength. In this case, known as Rayleigh scattering, the scattered (lost) power is roughly proportional to the $|E|^2$ at the scattering location and to the square of the scatterer's volume. The $|E|^2$dependence produces the same $1/R^3$ scaling for disorder-induced loss as for absorption loss, since disorder again

affects only the small fraction of the field inside the cladding where the interfaces or materials are.

2.7 Inter-modal coupling

Given the $1/R^3$ dependencies of the loss mechanisms described above, it may seem that increasing the core radius *R* is always a winning strategy. This is not the case. As *R* grows, we worsen losses and other problems due to inter-modal coupling: the transfer of energy from one mode to another at the same ω but different k_z. This is caused by fiber non uniformities that break the translational symmetry in *z*. This is a problem because higher-order modes will typically have higher losses (e.g., stronger penetration into the cladding), and will also produce modal dispersion. As we mentioned above, the differential losses of higher-order modes will suppress modal dispersion, but not if we couple into them faster than they are filtered out. Inter-modal coupling tends to worsen with increasing core radius *R*, for two reasons.

First, the number of core-guided modes increases. (The number of modes scales with the area $\sim R^2$.) Correspondingly, the mode spacing Δk_z decreases. This makes it easier for a non uniformity to couple different modes. Roughly speaking, $\pi/\Delta k_z$ is a minimum length scale for nonuniformities: if the fiber changes shape (e.g. due to ellipticity or stresses) over distances of this length scale or shorter, then coupling between modes may be substantial [32].

Second, even for a fixed Δk_z between modes, the inter-modal coupling due to fiber *bends* will worsen as *R* increases. Intuitively, as *R* grows, the difference in path length between the part of the core on the inside of the bend and the part on the outside will also grow. The result is a bigger "centrifugal force" that distorts the modes. The mathematical treatment of bending is rather complicated, and involves a coordinate transformation of the bent waveguide to a straight waveguide. However, the final result is elegant, and we summarize it here. If we take *x* to be the direction away from the center of the bend and $x = 0$ to be the center of the fiber at the bend radius R_b, the bend effectively adds a perturbation $\Delta\varepsilon$ and $\Delta\mu$ proportional to x/R_b. This acts like a potential ramp, analogous to a Stark effect in quantum mechanics, that pushes the fields towards the outside of the bend. Fiber performance then

deteriorates for two reasons. First, far enough away from the core, the exponential tails of the guided modes will "see" a perturbation so large that the band gap is shifted to a different frequency. This results in radiation losses that increase exponentially with $1/R_b$. Second, for sufficiently large R_b, the bend radiation is negligible, and instead the losses in high-contrast photonic-crystal fibers are dominated by coupling between guided modes [32]. This coupling varies as $(\frac{\mathrm{R}}{R_b})^2$ for large R_b (since R is the maximum value of x in the core), not including changes in Δk_z.

2.8 Dispersion properties of optical fibers

In optics, dispersion is the phenomenon in which the phase velocity of a wave depends on its frequency, or alternatively when the group velocity depends on the frequency. Media having such a property are termed dispersive media. Dispersion is sometimes called chromatic dispersion to emphasize its wavelength-dependent nature, or group-velocity dispersion (GVD) to emphasize the role of the group velocity.

The most familiar example of dispersion is probably a rainbow, in which dispersion causes the spatial separation of a white light into components of different wavelengths (different colors). However, dispersion also has an effect in many other circumstances: for example, GVD causes pulses to spread in optical fibers, degrading signals over long distances; also, a cancellation between group-velocity dispersion and nonlinear effects leads to soliton waves. Dispersion is most often described for light waves, but it may occur for any kind of wave that interacts with a medium or passes through an inhomogeneous geometry (e.g., a waveguide), such as sound waves [64].

There are generally two sources of dispersion: material dispersion and waveguide dispersion. Material dispersion comes from a frequency-dependent response of a material to waves. For example, material dispersion leads to undesired chromatic aberration in a lens or the separation of colors in a prism. Waveguide dispersion occurs when the speed of a wave in a waveguide (such as an optical fiber) depends on its frequency for geometric reasons, independent of any frequency dependence of the materials from which it is constructed. More generally, "waveguide" dispersion can occur for waves propagating through any inhomogeneous structure (e.g., a photonic crystal), whether or not the waves are confined to

some region. In general, both types of dispersion may be present, although they are not strictly additive. Their combination leads to signal degradation in optical fibers for telecommunications, because the varying delay in arrival time between different components of a signal "smears out" the signal in time.

2.8.1 Chromatic Dispersion (CD)

Chromatic dispersion is a broadening of the input signal as it travels down the length of the fiber. The concept to consider when talking about chromatic dispersion (CD) should be optical phase. It is important to mention optical phase before any explanations of CD or group delay because of their mathematical relationship. Group delay is defined as the first derivative of optical phase with respect to optical frequency [65]. Chromatic dispersion is the second derivative of optical phase with respect to optical frequency. These quantities are represented as follows:

Group Delay = $\partial\varphi / \partial\omega$

Chromatic Dispersion = $\partial^2\varphi / \partial\omega^2$

Where φ = optical phase and ω = optical frequency.

Chromatic dispersion consists of both material dispersion and waveguide dispersion as illustrated in Fig. 2.12.

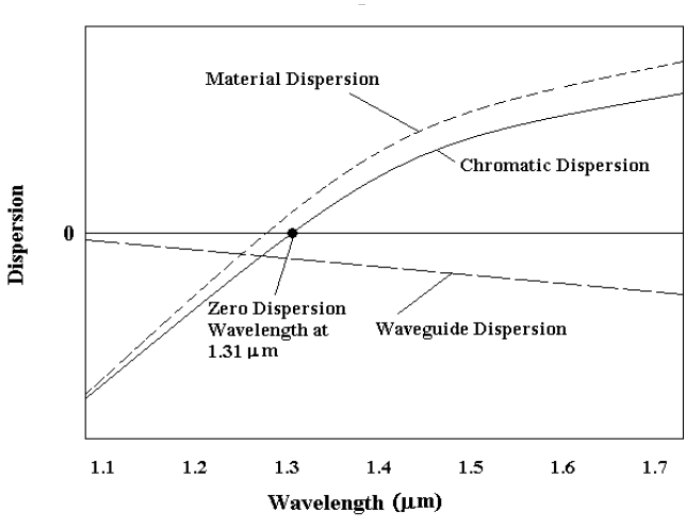

Fig. 2.12: Dispersion in a single mode optical fiber as a function of wavelength.

Both of these phenomena occur because all optical signals have a finite spectral width, and different spectral components will propagate at different speeds along the length of the fiber. One cause of this velocity difference is that the index of refraction of the fiber core is different for different wavelengths. This is called material dispersion and it is the dominant source of chromatic dispersion in single-mode fibers. Another cause of dispersion is that the cross-sectional distribution of light within the fiber also changes for different wavelengths. Shorter wavelengths are more completely confined to the fiber core, while a larger portion of the optical power at longer wavelengths propagates in the cladding. Since the index of the core is greater than the index of the cladding, this difference in spatial distribution causes a change in propagation velocity. This phenomenon, illustrated in Fig. 2.13, is known as waveguide dispersion. Waveguide dispersion is relatively small compared to material dispersion [65].

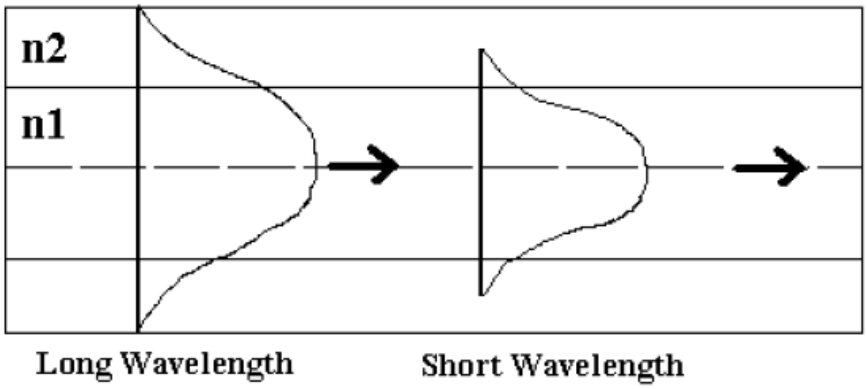

Fig. 2.13: Waveguide dispersion- different wavelengths will experience different effective refractive index.

Chromatic dispersion in a component is significantly different than chromatic dispersion in long length optical fiber. Chromatic dispersion remains constant over the bandwidth of a communications channel for long lengths of fiber. As a result, chromatic dispersion is a poor predictor of component performance in a communications system.

Chromatic dispersion can cause bit errors in digital communications or distortion and a higher noise floor in analog communications, and can pose a serious issue in high-bit-rate

systems if it is not measured accurately and some form of dispersion compensation is not employed.

2.8.2 Group Velocity Dispersion (GVD)

Another consequence of dispersion manifests itself as a temporal effect. The formula v = c / n calculates the phase velocity of a wave; this is the velocity at which the phase of any one frequency component of the wave will propagate. This is not the same as the group velocity of the wave, that is the rate at which changes in amplitude (known as the envelope of the wave) will propagate. For a homogeneous medium, the group velocity v_g is related to the phase velocity by (here λ is the wavelength in vacuum, not in the medium)

The group velocity v_g is often thought of as the velocity at which energy or information is conveyed along the wave. In most cases this is true, and the group velocity can be thought of as the signal velocity of the waveform. In some unusual circumstances, called cases of anomalous dispersion, the rate of change of the index of refraction with respect to the wavelength changes sign, in which case it is possible for the group velocity to exceed the speed of light ($v_g > c$). Anomalous dispersion occurs, for instance, where the wavelength of the light is close to an absorption resonance of the medium. When the dispersion is anomalous, however, group velocity is no longer an indicator of signal velocity. Instead, a signal travels at the speed of the wave front, which is c irrespective of the index of refraction. Recently, it has become possible to create gases in which the group velocity is not only larger than the speed of light, but even negative. In these cases, a pulse can appear to exit a medium before it enters. Even in these cases, however, a signal travels at, or less than, the speed of light, as demonstrated by Stenner [64].

The group velocity itself is usually a function of the wave's frequency. This results in group velocity dispersion (GVD), which causes a short pulse of light to spread in time as a result of different frequency components of the pulse travelling at different velocities. GVD is often quantified as the group delay dispersion parameter (again, this formula is for a uniform medium only):

$$D = -\frac{\lambda}{c}\frac{d^2 n}{d\lambda^2}. \tag{2.20}$$

If D is less than zero, the medium is said to have positive dispersion. If D is greater than zero, the medium has negative dispersion. If a light pulse is propagated through a normally dispersive medium, the result is the higher frequency components travel slower than the lower frequency components. The pulse therefore becomes positively chirped, or up-chirped, increasing in frequency with time. Conversely, if a pulse travels through an anomalously dispersive medium, high frequency components travel faster than the lower ones, and the pulse becomes negatively chirped, or down-chirped, decreasing in frequency with time.

The result of GVD, whether negative or positive, is ultimately temporal spreading of the pulse. This makes dispersion management extremely important in optical communications systems based on optical fiber, since if dispersion is too high, a group of pulses representing a bit-stream will spread in time and merge together, rendering the bit-stream unintelligible. This limits the length of fiber that a signal can be sent down without regeneration. One possible answer to this problem is to send signals down the pcf at a wavelength where the GVD is zero (e.g., around 1.3–1.5 μm in silica), so pulses at this wavelength suffer minimal spreading from dispersion—in practice, however, this approach causes more problems than it solves because zero GVD unacceptably amplifies other nonlinear effects (such as four wave mixing). Another possible option is to use soliton pulses in the regime of anomalous dispersion, a form of optical pulse which uses a nonlinear optical effect to self-maintain its shape solitons have the practical problem, however, that they require a certain power level to be maintained in the pulse for the nonlinear effect to be of the correct strength. Instead, the solution that is currently used in practice is to perform dispersion compensation, typically by matching the fiber with another fiber of opposite-sign dispersion so that the dispersion effects cancel; such compensation is ultimately limited by nonlinear effects such as self-phase modulation, which interact with dispersion to make it very difficult to undo.

Dispersion control is also important in lasers that produce short pulses. The overall dispersion of the optical resonator is a major factor in determining the duration of the pulses emitted by the laser. A pair of prisms can be arranged to produce net negative dispersion, which can be used to balance the usually positive dispersion of the laser medium. Diffraction gratings can also be used to produce dispersive effects; these are often used in high-power laser amplifier systems. Recently, an alternative to prisms and gratings has been developed:

chirped mirrors. These dielectric mirrors are coated so that different wavelengths have different penetration lengths, and therefore different group delays. The coating layers can be tailored to achieve a net negative dispersion.

2.8.3 Waveguides Dispersion

Optical fibers, which are used in telecommunications, are among the most abundant types of waveguides. Dispersion in these fibers is one of the limiting factors that determine how much data can be transported on a single fiber.

The transverse modes for waves confined laterally within a waveguide generally have different speeds (and field patterns) depending upon their frequency (that is, on the relative size of the wave, the wavelength) compared to the size of the waveguide.

In general, for a waveguide mode with an angular frequency $\omega(\beta)$ at a propagation constant β (so that the electromagnetic fields in the propagation direction (z) oscillate proportional to $e^{i(\beta z - \omega t)}$), the group-velocity dispersion parameter D is defined as:

$$D = -\frac{2\pi c}{\lambda^2}\frac{d^2\beta}{d\omega^2} = \frac{2\pi c}{v_g^2\lambda^2}\frac{dv_g}{d\omega} \tag{2.21}$$

Where $\lambda = 2\pi c / \omega$ is the vacuum wavelength and $v_g = d\omega / d\beta$ is the group velocity. This formula generalizes the one in the previous section for homogeneous media, and includes both waveguide dispersion and material dispersion.

A similar effect due to a somewhat different phenomenon is modal dispersion, caused by a waveguide having multiple modes at a given frequency, each with a different speed. A special case of this is polarization mode dispersion (PMD), which comes from a superposition of two modes that travel at different speeds due to random imperfections that break the symmetry of the waveguide.

2.8.4 Polarization Modal Dispersion

Finally, another important form of inter-modal coupling is known as polarization-mode dispersion (PMD). PMD arises in an ordinary fiber because the operating mode is doubly

degenerate, with two orthogonal polarizations. Any imperfection or stress in the fiber, however, can break the symmetry and split these two polarizations into modes that travel at different speeds. This produces a form of modal dispersion, where pulses spread due to random imperfections in the fiber [32]. The same thing can happen in a photonic-crystal fiber if we operate in a doubly degenerate mode. The differential losses of a hollow-core fiber, however, allow one to operate in a low-loss higher-order mode like te01 that is non degenerate and hence immune to PMD (no perturbation can split the mode into two). Alternatively, one can design a core that is so asymmetric that it supports only a single non degenerate mode.

Chapter 3

Literature Survey

3.1 Philip Russell et. all. 2003 [66]

Photonic crystal fibers have been the focus of increasing scientific and technological interest since the first working example was reported in 1996. Although superficially similar to a conventional optical fiber, PCF has a unique microstructure, consisting of an array of microscopic holes (or channels) that runs along the entire length of the fiber. These holes act as optical barriers or scatterers, which suitably arranged can "corral" light within a central core (either hollow or made of solid glass). The holes can range in diameter from -25 nm to -50 pm. Although most PCF is formed in pure silica glass, it has also recently been made using polymers and non-silica glasses, where it is difficult to find compatible core and cladding materials suitable for conventional total internal reflection guidance. PCF supports two guidance mechanisms: total internal reflection, in which case the core must have a higher average refractive index than the holey cladding; and a two-dimensional photonic bandgap, when the index of the core is uncritical - it can be hollow or filled with material. Light can be controlled and transformed in these fibers with unprecedented freedom, allowing for example the guiding of light in a hollow core, the creation of highly nonlinear solid cores with anomalous dispersion in the visible and the design of fibers that support only one transverse spatial mode at all wavelengths. Applications are emerging in many diverse areas of science and technology.

3.2 Frederic GEROME, Jean-huh AUGUSTE, Jean-Marc BLONDY et. all. 2003 [67]

A photonic crystal fiber (PCF) design based on a particular periodic arrangement of air holes for chromatic dispersion compensation has been demonstrated. A two concentric cores structure is formed and exhibits very high negative chromatic dispersion.

3.3 Knnimasa Saitoh and Masanori Koshiba et. all. 2003 [68]

In conventional photonic crystal fibers (PCFs), the cladding structure is usually arrayed with the same diameter of air holes in a regular oriented triangular lattice. However, in index-guiding PCFs, the periodicity in the cladding region is not required to confine the light into

the high-index core region. In this paper, report has been proposed that by varying the hole diameter of each air-hole ring along the radius, it is possible to control chromatic dispersion of index guiding PCFs in wide wavelength range. Using this design principle, a PCF design with ultra-low and ultra flattened dispersion is achieved through a full-vector finite element method with anisotropic perfectly matched layers. Effective mode areas and leakage loss properties are also investigated and cited**.**

3.4 F. Poli, A. Cucinotta, S. Selleri, and A. H. Bouk et. all. 2004 [69]

The dispersion properties of large-hole photonic crystal fibers (PCFs) are tailored by varying the diameter of the air-holes of the first three rings so as to obtain fibers with a small effective area and low dispersion values in a wide wavelength range close to1550 nm. Highly nonlinear triangular PCFs with effective area of a few square micrometers, flattened dispersion curve and zero-dispersion wavelength close to 1500 nm have been designed and demonstrated.

3.5 Takashi Matsui, Jian Zhou, Kazuhide Nakajima, and Izumi Sankawa et. all. 2005 [70]

Flat dispersion can be realized with photonic crystal fibers (PCF) a over a wide wavelength range that cannot be obtained with a conventional single-mode fiber. However, the confinement loss tends to increase as a result in a conventional dispersion-flattened PCF (DF-PCF) that has uniform air holes. In this paper, a novel PCF that has two cladding layers with different effective indices is anticipated. The authors numerically showed that the proposed PCF can achieve an ultralow dispersion variation of less than 0.8 ps/nm.km in all telecommunication bands, with a large effective area greater than 100 μm2 and a low confinement loss less than 0.01 dB/km.

3.6 Arismar Cerqueira S. Jr.* and K. Z. Nobregat et. all. 2005 [71]

Chromatic dispersion engineering is one of the most promising advantages highlighted by the use of photonic crystal fibers, PCFs. Its two-dimensional photonic crystal structure allows managing the waveguide dispersion as a function of the their design parameters such as: inter-hole spacing, hole diameter, number of air rings and cladding refractive index. Most PCFs are silica-based with a honeycomb cladding. This paper represents a dispersion design

methodology of high-index glass photonic crystal fibers based on a new-geometry with numerical results pointing out at positive or nearly zero ultra flattened dispersion in a wide wavelength window. The nearly zero case presents chromatic dispersion at λ = 1.55 μm, m equal to -0.352 $ps/km/nm$ and a low slope equal to 1.10^{-3} $ps/nm^2/km$ at 1.5-1.6 μm range. The lowest obtained slope was 5. 10^{-4} $ps/nm^2/km$

3.7 Niels Asger Mortensen et. all. 2006 [72]

In this paper, we consider photonic crystal fibers (PCFs) made from arbitrary base materials with the introduction of short-wavelength approximation which permits a mapping of the Maxwell's equations onto a dimensionless eigenvalue equations that has the form of the famous Schrödinger equation in quantum mechanics. The mapping paves a way for an entire analytical solution of the dispersion problem that is in qualitative agreement with plane-wave simulations of the Maxwell's equations for large-mode area PCFs. Paper offered a new angle on the foundation of the eternally single-mode property and showed that PCFs continuously provides single mode results for a normalized air-hole diameter smaller than 0.42, independent of the base material. Finally, we showed how the group-velocity dispersion relates merely to the geometry of the photonic crystal cladding.

3.8 A. Kudlinski, A. K. George et. all. 2006 [73]

We have fabricated a photonic crystal fiber with a continuously decreasing zero-dispersion wavelength along its length. It has been used to generate an ultraviolet-extended super continuum from a nanosecond pump source at 1.064 μm.

3.9 Federica Poli, Annamaria Cucinotta et. all. 2008 [74]

Through different analysis results, it is demonstrated the effectiveness of the finite element method as a numerical tool to accurately analyze the properties of both solid core and hollow core photonic crystal fibers.

3.10 Sh. Mohammad Nejad, M. Aliramezani et. all. 2008 [75]

A novel photonic crystal fiber (PCF) structure with triangular core is proposed. The PCF has ultra-flattened dispersion and negligible loss characteristics throughout the telecommunication windows (1.2 to 1.7 μm). The design strategy to achieve these properties is based on optimization of three air-hole diameters. Furthermore, the PCF has only seven

rings of air-holes to control loss. The validation of the proposed design is carried out by employing a 2-D FDTD with perfectly matched layers. Macro-bending loss performance of the designed PCF is also studied. It is found that the fiber shows low bending losses for the smallest feasible bending radius of 5mm.

3.11 Takashi Matsui, Kazuhide Nakajima et. all. 2009 [76]

We discuss the applicability of photonic crystal fiber (PCF) with a uniform air-hole structure to high-speed and wide-band transmission over conventional telecommunication bands. We design the PCF to maximize the effective area by utilizing the macro-bending losses of the fundamental and first higher order modes (HOM) and clarify that a single-mode and low bending loss PCF can realize the largest effective areas of 133 and 157 m□ for transmission over the 1260–1625 nm and 1460–1625 nm wavelength ranges, respectively. We then investigate the impact of the designed PCF on nonlinearity reduction over a wide wavelength range and show that the PCF helps to increase the maximum channel power in a wavelength division multiplexing system. We also discuss the distributed Raman amplification (DRA) characteristics of PCF with a large effective area. Our results show that we can expect to improve the signal to noise ratio with DRA in spite of the low nonlinearity of the designed PCF. Dispersion compensating fiber (DCF) with a conventional W-shaped index profile is designed to compensate for the relatively large dispersion of the PCF, and we show that the designed DCF can extend the dispersion compensation bandwidth from 1340 nm to 1650 nm for a 40 Gbit/s transmission. Finally, we clarify the applicability of the large effective area PCF with the uniform air-hole structure as a high-speed and wide-band transmission medium.

3.12 Nihal F. F. Areed land Hamdy Elmikati et. all. 2009 [77]

A full vectorial Finite Difference Frequency Domain (FDFD) analysis is effectively applied to investigate the modal characteristics of photonic crystal fibers (PCFs). Comparison with a Full Vectorial Imaginary Distance Beam Propagation (FVIDBP) method based on finite element scheme is made and excellent agreement is achieved. Moreover, a detailed study of PCF with hexagonal array of holes has been carried out with the purpose of optimizing both the leakage loss and the chromatic dispersion.

3.13 Uma R. Rao, B. K. Lande et. all. 2009 [78]

High data rate demand on optical fiber networks is ever increasing and in practical dispersion is the major limiting factor that provides obstacles in achieving high data rates. Present day dense wavelength division multiplexing (WDM) networks need very rigorous dispersion management criteria. With commercial deployment of optical fiber links in the two decades, dispersion phenomenon is well understood and different methods for skirmishing the pulse spreading due to dispersion are invented and developed. In the recent years, a special class of optical fibers known as photonic crystal fibers (PCF) is widely being explored for its dispersion compensating properties. PCFs offer a very large negative dispersion which can be readily varied by changing their design geometry and this paper represents two PCF designs that elaborates the large negative chromatic dispersion offered by them.

3.14 Mohamed Farhat O. Hameed, Salah S. A. Obayya et. all. 2009 [79]

Modal analysis of an index guiding soft glass photonic crystal fiber infiltrated with a nematic liquid crystal (NLC-PCF) has been depicted in this paper. The analysis is carried out by using the full vectorial finite difference method that is capable of dealing perfectly with anisotropic waveguide problems. The analyzed parameters are the effective index, birefringence, dispersion, effective mode area, and confinement losses for the two fundamental polarized modes. Investigation of the effects of the structure geometrical parameters, rotation angle of the director of the NLC and temperature on the modal properties is done. Numerical results reveal that the proposed structure offers high birefringence of 0.012 at the operating wavelength 1.55μm with low losses for the two polarized modes. In addition, the design is tailored to obtain a flat dispersion over a wide range of wavelengths with high Birefringence.

3.15 Arismar Cerqueira S Jr et. all. 2010 [80]

Photonic crystal fibers present a wavelength-scale periodic microstructure running along their length. Their core and two-dimensional photonic crystal might be based on varied geometries and materials, enabling light guidance due to different propagation mechanisms in an extremely large wavelength range, extending to the terahertz regions. As a result, these fibers have revolutionized the optical fiber technology by means of creating new degrees of freedom in the fiber design, fabrication and applicability. This report aims to provide a

detailed statement on the recent progress and novel potential applications of photonic crystal fibers.

3.16 Sandhir K Singh, Dharmendra K Singh et. all. 2010 [81]

A photonic crystal fiber (PCF) allows a new way to confine light in fibers. The periodic air holes in the fiber works as a cladding, but provides much more flexibility and efficiency in the design. Plane-wave expansion technique for generating and analyzing photonic band structures is presented in this work. Hexagonal periodic cross-section of air holes with a simple 2D XY array in a silicon fiber is analyzed for calculating parameters such as mode effective index, dispersion and single mode operation over wide wavelength range. The results of this design sample are presented in this paper, showing the better result to analyze this new class of fiber. PCF can be used for biomedical application, spectroscopy, and super continuum generation.

3.17 Saeed Olyaee and Fahimeh Taghipour et. all. 2011 [82]

Low and ultra-flattened dispersion is extremely desirable in transmission medium for wavelength-division-multiplexing (WDM) systems and PCF offered great help in this direction. Again low confinement losses as well as a large effective area in a wide range of wavelengths are also desirable factors. Relatively low dispersion with negligible variation has become feasible in the wavelength range of 1.1 to 1.8μm through the proposed design in this article. According to this new structure of PCF presented in this paper, the dispersion slope is 6.8×$10^{-4} ps/km/nm^2$ and the confinement loss reaches below 10^{-6} dB/km in this range have been achieved, while at the same time an effective area of more than 50μm^2 has been attained. For the analysis of this PCF, finite-difference time-domain (FDTD) method with the perfectly matched layers (PML) boundary conditions has been used.

3.18 Nagesh Janrao et. all. 2011 [83]

In recent years photonic crystal fibers (PCFs) made of silica and air hole has provided a new approach for dispersion compensation. For dispersion compensating fibers, large negative dispersion D (ps/km-nm) is required. The refractive index profile of conventional, step-index, dispersion compensation fiber can be changed in order to obtain high waveguide dispersion, however, this needs high doping, giving rise to higher losses. PCFs are now being

increasingly used as an alternative approach to dispersion compensation. This paper proposes a new geometry of PCFs, which uses 'square' holes instead of circular holes, which gives large negative dispersion without high doping. Dispersion compensating photonic crystal fiber is designed with square holes with equivalent width w given as d=1.128w where w=width of square holes in PCF and d is diameter of circular holes in more conventional PCF. This relation is newly introduced between circular diameter and square width of air holes.

Chapter 4

Simulation and Results

4.1 Structure of photonic Crystal Fiber

Design of PCF consists of a solid core of silica with a periodic array of air holes running along the length of the fiber acting as the cladding. In this type of PCF the mean cladding refractive index is lower than the core index. This type of fiber works on the principle of modified total internal reflection. In particular, design and construction of photonic crystals can be done with photonic band gaps that prevents light from propagating in certain directions with specified frequencies (i.e., a certain range of wavelengths, or "colors," of light). As the operation is based on modified total internal reflection, the properties of high index core triangular PCFs in many respects resemble those of step index fibers.

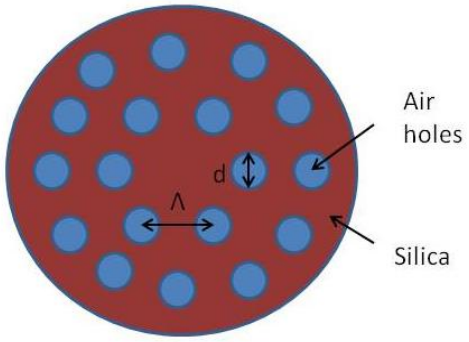

Fig. 4.1: photonic crystal fiber with a triangular lattice of air holes, where d is the hole diameter, Λ is the hole pitch, and the refractive index of silica (n) is 1.4. In the centre, an air hole is omitted creating a central high index defect serving as the fiber core.

The cross-sectional view of the proposed PCF design is shown in Fig. 4.1. The cladding of the PCF consists of a hexagonal lattice of circular air holes with a diameter d in fused silica. In the centre, an air hole is omitted creating a central high index defect serving as the fiber core.

Basic working of pcf does depend upon two modes, namely single mode and multi mode. In multi mode pcf, instead of core the light is confined in both core and cladding due to the effect of hole pitch, diameter of air holes and the number of layers of air holes. Propagation

of electric field distribution in multi mode pcf has been shown in Fig. 4.2. But due to certain difficulties the multi mode provides undesired results in the photonic crystal fiber case.

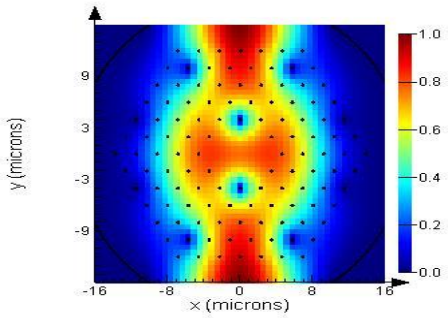

Fig.4.2: Electric field distribution in multi mode photonic crystal fibers.

The defect in the center acting as the core disturbs the periodicity of holes that helps in obtaining strong optical confinement in the core as shown in the Fig. 4.3. The periodic structure (air holes) surrounding the defect core causes a collective cancellation of scattering of light leading to localization of light in the defect region. Fig. 4.3 shows a strong optical confinement in defect core where core radius (a) = 2.78 µm, N= 8, n=1.4, d=.44 µm, Λ=1.5 µm.

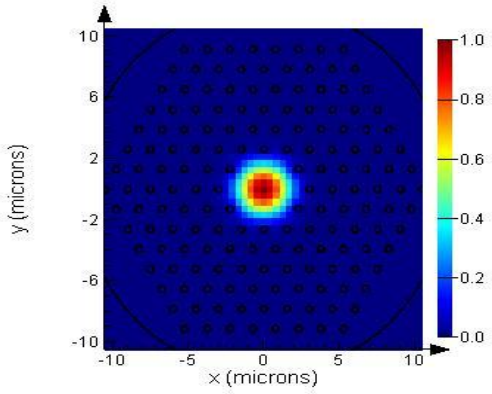

Fig. 4.3: Electric field distribution in the single mode photonic crystal fiber with core radius (R) = 2.78 µm, N= 8, n=1.4, d=.44 µm, Λ =1.5 µm.

In single mode pcf light is totally confined in the core enabling various advantages such as low confinement loss, low scattering, low dispersion loss, low bending loss when compared with multi mode pcfs. Due to above qualities, single mode photonic crystal fibers have been taken into account in this thesis report. Fig. 4.3 represents the propagation of electric field distribution in single mode PCFs.

4.2 Effects of different parameters on photonic crystal fiber:

4.2.1 Variation of effective index versus diameter of air holes at different hole pitch:

Fig. 4.4 shows the variations of effective index of pcf with the diameter of air holes (d) for various values of lattice constant (Λ). It can be concluded that effective index decreases as diameter of air holes (d) increases as a whole. For low values of diameter of air holes, periodicity effect doesn't support its function, as fluctuations can be observed for hole pitch values of 3 and 3.5μm. As the diameter reaches value of 0.9μm and beyond effective index is almost constant as periodicity truly define its purpose thereafter.

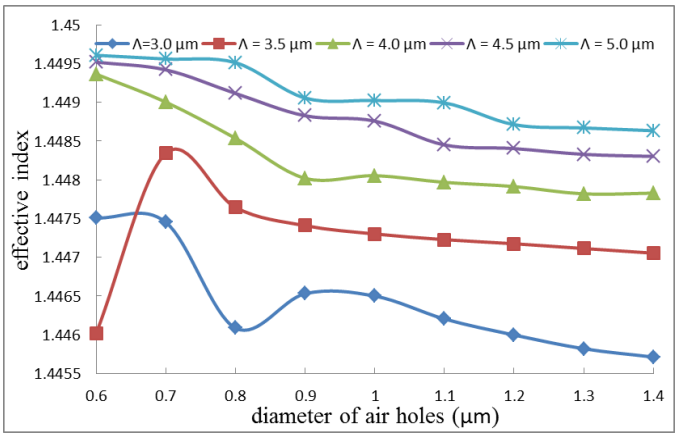

Fig.4.4: Effect of diameter on effective index at various versus radius of air holes at different hole pitch, N=8, n=1.45, λ=1.55 μm.

4.2.2 Effect on dispersion by various parameters:

4.2.2.1 Variation of dispersion versus diameter of air holes for different values of hole pitch (Λ):

Fig. 4.5 shows variations in waveguide dispersion with diameter of air holes for different values of hole pitch. It can be seen that waveguide dispersion becomes more negative initially with increasing hole diameter. With further increase in the value of d, it attains a maximum value in negative direction and increases in positive direction afterwards.The optimised value obtained for waveguide dispersion is -31.6 ps/km/nm at d=0.44 μm, Λ=1.5 μm where the operating wavelength is 1.55 μm.

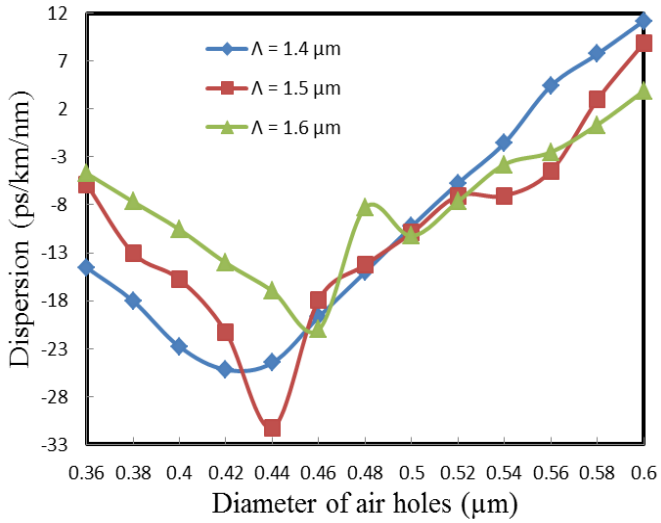

Fig. 4.5: Effect of diameter of air holes(d) on the Dispersion at different values of hole pitch (Λ), N=8, n=1.4, λ=1.55 µm.

4.2.2.2Variation of dispersion versus number of air holes layers (N)

In Fig. 4.6 the effect of number of air-holes layers on waveguide dispersion has been shown. Initially dispersion increases in negative direction as N increases up to the value of 4 and in the mean while dispersion changes its sign from negative to positive, at N=3 its layers does not support periodicity due to that optical confinement is not good and light is also leaking in to the cladding. As we tend to increase N to higher values the periodicity supports the optical confinement and the waveguide dispersion increases negative and we get the largest negative value of waveguide dispersion as -31.6 ps/km/nm at N=8. At N=8, layers periodicity effects best and if N increases there is no effect on the optical confinement and further waveguide dispersion increases at an alarming rate and it behave as a conventional fiber. As more negative the waveguide dispersion it compensates the more positive material dispersion and optical signal is transmit to the long distances.

4.2.2.3 Variation of dispersion versus wavelength(λ) for various values of refractive index(n) of the core:

In addition, different glasses (refractive indices) can also be exploited, since in this way both waveguide dispersion and material dispersion can be tailored. Fig 4.9 presents a comparison between two PCFs for identical geometric parameters, 8 layers, d=0.44 µm, Λ=1.5 µm and λ=1.5 µm, but with different core materials: (n=1.4) and (n=1.6). It can be seen from that

negative dispersion increases as wavelength increases for different values of refractive index. Although we get largest negative value of dispersion at n=1.6 beyond λ=1.8 μm point but dispersion is constantly low for n=1.4 for the major part of graph. As we increases the refractive index (n) the negative peak is shifted towards the longer wavelength and optical communication is dealing near the λ=1.55 μm, hence choice of selecting n=1.4 for this thesis was quiet obvious.

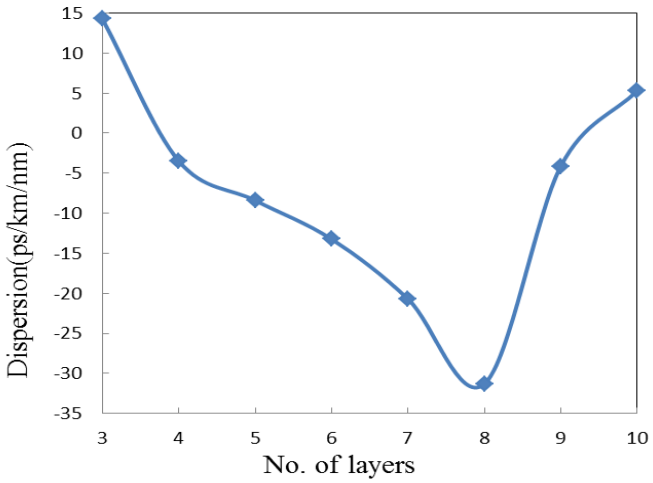

Fig. 4.6: Effect of number of layers(N) on the dispersion at n=1.4, λ=1.55 μm, Λ=1.5 μm, d=0.44 μm .

4.2.2.4 Polarization Dependence of Proposed PCF

Modal birefringence and Polarization Dependent Loss (PDL) are very important parameters for the optical communication. So control of these parameters is very necessary. The variation on the modal birefringence and polarization dependent loss with diameter of air holes are shown in Fig. below. Fig. 4.7 demonstrate variation in the value of modal birefringence with diameter (d) for different values of hole pitch (Λ). With initial increase in diameter, all the curves varies in pulsating manner around zero modal line but as the value of d pass 1.3 μm mark, most of the curves undergoes low values that are close to zero modal line and continues to follow this nature as value of d reaches up to the range of 2.2 μm. Fig. 4.8 shows the variation of polarization dependent loss (PDL) with diameter of air holes (d) at the value of hole pitch (Λ) = 3.0μm. Except with an intial dip at d =0.9μm, curve is almost constant for a major part of the Fig. As shown in Fig. PDL is acceptably small for a wide range of hole diameter. Low modal birefringence on the order of 10^{-4} and low polarization dependent loss on the order of 10^{-14} is realized with the proposed PCF structure.

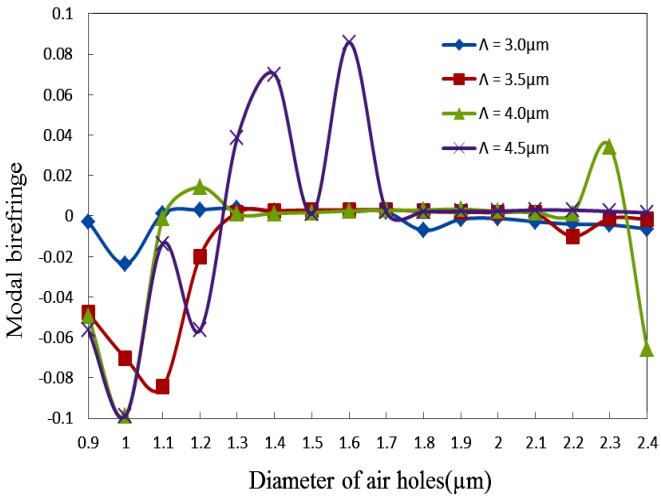

Fig.4.7: Variation on modal birefringence with diameter of air holes (d) for different values of hole pitches (Λ) at N=8, n=1.4, λ =1.5 µm.

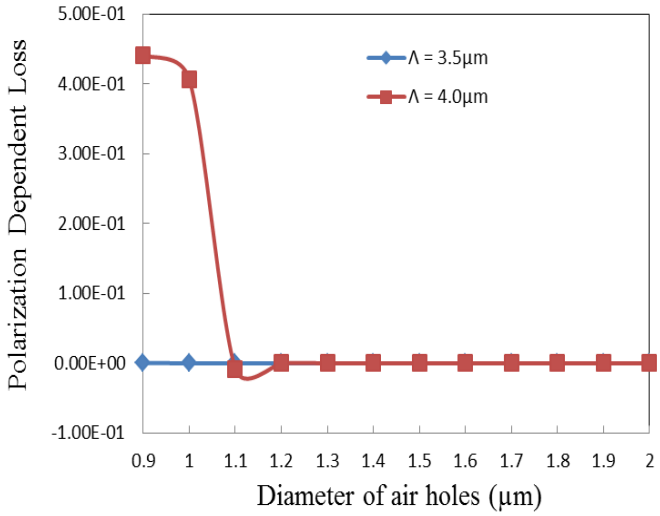

Fig. 4.8: Variation on the Polarization Dependent Loss (PDL) with diameter of air holes (d) at different hole pitch (Λ) at N=8, n=1.4, λ =1.5 µm.

4.2.2.5 Variation of dispersion versus wavelength(λ) for various values of diameter of the air holes(d):

The optimized PCFs have been designed by taking into account the effects provided by the increase of refractive index step and the suitable choice of PCF design parameters (number of air holes rings, hole sizes and inter-hole spacing) and all the calculated profiles have been depicted in Table 4.1. It has been proposed a eight ring PCF with refractive index 1.4 and

hole pitch of 1.5 μm for all the profiles. Profile no.1 provides maximum dispersion in the largest possible wavelength window of 1.47 to 1.91μm, in which the dispersion varies from -15.0 to – 14.79 ps/nm/km, providing a slope equal to $4.77x10^{-4}$ ps/km^2/nm at d= 0.40 μm. For profile 2 with d= 0.42 μm low ultra flattened dispersion in a range of -20.35 to – 20.12 ps/nm/km with dispersion slope equal to $5.47\ x10^{-4}$ ps/km^2/nm has been achieved within the wavelength range of 1.49 to 1.91 μm. Largest negative ultra flattened dispersion ranging from -31.65 to -31.30

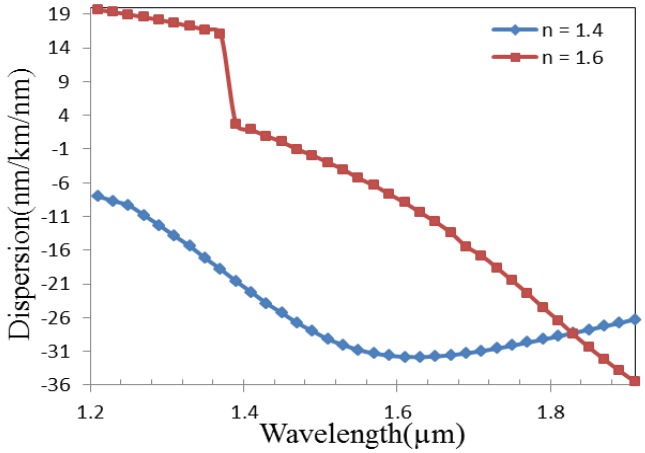

Fig. 4.9: Variation of wavelength(λ) on dispersion at varius values of refractive index(n), N=8, d=0.44 μm, Λ=1.5 μm, λ =1.5 μm.

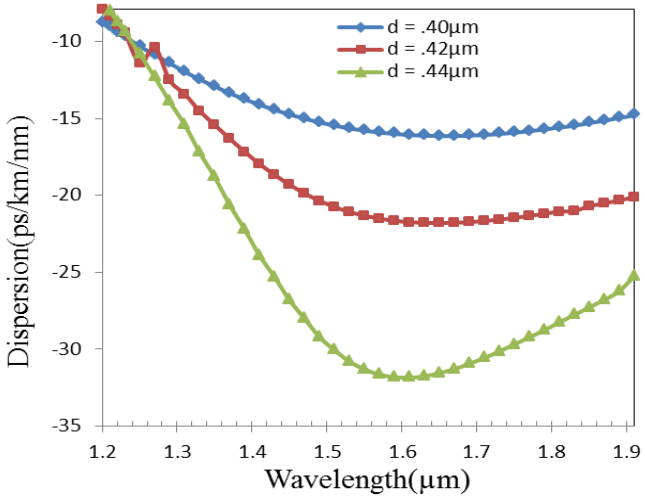

Fig. 4.10: Variation of wavelength(λ) on dispersion at varius values of diameter of air holes(d), N=8, n=1.4, Λ=1.5 μm, λ =1.5 μm.

Profiles	Diameter of air holes (μm)	Dispersion range (ps/km/nm)	Dispersion slope (ps/ km.nm^2)	Wavelength range (μm)
1.	0.40	- 15.0 to – 14.79	4.77×10^{-4}	1.47 to 1.91
2.	0.42	-20.35 to – 20.12	5.47×10^{-4}	1.49 to 1.91
3.	0.44	-31.65 to -31.30	3.50×10^{-3}	1.57 to 1.67

Table 4.1 Showing various PCF profiles with Number of layers (N) = 8, Lattice constant (Λ) = 1.5μm, Refractive index (n) = 1.4.

ps/nm/km has been achieved with profile 3 for which dispersion slope touching the value of -3.50×10^{-3} ps/km^2/nm within the minimum wavelength window of 1.57 to 1.67 μm. Thus a trade off has been done between low dispersion value and large wavelength range. Hence profile 2 provided the most suitable results with low flattened dispersion with respect to profile 1 and large wavelength window compared to profile 3.

Chapter 5

Conclusions

This thesis targets at the design and simulation of silica solid-core photonic band gap fibers with large waveguide dispersion and ultra-flat dispersion. A detailed numerical study on the impact of the core geometry on the transmission performance of realistic solid-core fibers designs was carried out. Modal birefringence and polarization dependent loss values were also calculated to analyses the structure more accurately.

An easy-to-implement design of PCF with large waveguide dispersion and a small dispersion slope has been proposed .The dispersion properties of PCF are tailored with simple structural variations in PCF such as refractive index step, number of air holes rings, hole sizes and inter-hole spacing and all the calculated profiles have been depicted in Table 1. It has been proposed a eight ring PCF with refractive index 1.4 and hole pitch of 1.5μm for all the profiles. Profile number1 with d=0.40μm, provides maximum dispersion in the largest possible wavelength window of 1.47 to 1.91μm, in which the dispersion varies from -15.0 to – 14.79 ps/nm/km, providing a slope equal to $4.77x10^{-4}$ ps/nm^2/km. For profile 2 with d=0.42μm, low ultra flattened dispersion in a range of -20.35 to – 20.12 ps/nm/km and dispersion slope of $5.47x10^{-4}$ ps/nm^2/km have been achieved within the wavelength range of 1.49 to 1.91μm. Largest negative ultra flattened dispersion ranging from -31.65 to -31.30 ps/nm/km has been achieved with profile 3, for which dispersion slope touched the value of -$3.50x10^{-3}$ps/nm^2/km within the minimum wavelength window of 1.57 to 1.67μm. Thus a tradeoff has been done between low dispersion value and large wavelength range. Hence profile 2 provided the most suitable results with low flattened dispersion with respect to profile 1 and large wavelength window as compared to profile 3. Modal birefringence remains on the order of 10^{-4} and polarization dependent loss touched the range of 10^{-13} to 10^{-14} constantly during designing and simulation purpose for this thesis.

The proposed design is easy to implement because of the simplicity of structural variation of PCF and it can be used to compensate dispersion and dispersion slope in the long-haul optical fiber links and sensors.

References

[1] P. Russell, “Photonic crystal fibers,” Science, 299(5605), 358–362, 2003.

[2] P. S. J. Russell, “Photonic-crystal fibers,” Journal of Lightwave Technology, 24(12), 4729–4749, 2006.

[3] P. Kaiser, E. A. J. Marcatili, and S.E. Miller, “A new optical fiber,” Bell Systems Technical Journal, 52(2), 265–269, 1973.

[4] P. Kaiser and H. W. Astle, “Low-loss single material fibers made from pure fused silica,” Bell Systems Technical Journal, 53, 1021–1039, 1974.

[5] J. B. MacChesney, P. B. O’Connor, and H. M. Presby, “A new technique for preparation of low-loss and graded index optical fibers,” Proceedings of the IEEE, 62, 1278–1279, 1974.

[6] W. G. French, J. B. Macchesney, and A. D. Pearso, “Glass fibers for optical communications,” Annual Review of Materials Science, 5, 373–394, 1975.

[7] W. Hermann and D. U. Wiechert, “Refractive-index of doped and undoped pcvd bulk silica,” Materials Research Bulletin, 24(9), 1083–1097, 1989.

[8] G. P. Agrawal, “Nonlinear fiber optics,” Academic Press, San Diego, 3rd edition, 2001.

[9] S. R. Nagel, J. B. Macchesney, and K. L. Walker, “An overview of the modified chemical vapor-deposition (MCVD) process and performance,” IEEE Journal of Quantum Electronics, 18(4), 459–476, 1982.

[10] T. A. Birks, P. J. Roberts, P. S. J. Russell, D. M. Atkin, and T. J. Shepherd, “Full 2-D photonic bandgaps in silica/air structures,” Electronics Letters, 31(22), 1941–1943, 1995.

[11] J. C. Knight, “Photonic crystal fibers,” Nature, 424(6950), 847–851, 2003. 124

[12] J. C. Knight, T. A. Birks, P. S. Russell, and D. M. Atkin, “All-silica single-mode optical fiber with photonic crystal cladding,” Optics Letters, 21(19), 1547–1549, 1996.

[13] T. A. Birks, J. C. Knight, and P. S. Russell, “Endlessly single-mode photonic crystal fiber,” Optics Letters, 22(13), 961–963, 1997.

[14] R. F. Cregan, B. J. Mangan, J. C. Knight, T. A. Birks, P. S. Russell, P. J. Roberts, and D. C. Allan, “Single-mode photonic band gap guidance of light in air,” Science, 285(5433), 1537–1539, 1999.

[15] B.J. Mangan, L. Farr, A. Langford, P.J. Roberts, D.P. Williams, F. Couny, M. Lawman, M. Mason, S. Coupland, R. Flea, H. Sabert, T.A. Birks, J.C. Knight, and P.St.J. Russell, "Low loss (1.7 db/km) hollow core photonic bandgap fiber," Optical Fiber Communication Conference, 2(3), 2004.

[16] R. Amezcua-Correa, F. Gerome, S. G. Leon-Saval, N. G. R. Broderick, T. A. Birks, and J. C. Knight, "Control of surface modes in low loss hollow-core photonic bandgap fibers," Optics Express, 16(2), 1142–1149, 2008.

[17] J. K. Ranka, R. S. Windeler, and A. J. Stentz, "Visible continuum generation in air-silica microstructure optical fibers with anomalous dispersion at 800 nm," Optics Letters, 25(1), 25–27, 2000.

[18] M. D. Nielsen and N. A. Mortensen, "Photonic crystal fiber design based on the V – parameter," Optics Express, 11(21), 2762–2768, 2003.

[19] D. Mogilevtsev, T. A. Birks, and P. S. Russell, "Group-velocity dispersion in photonic crystal fibers," Optics Letters, 23(21), 1662–1664, 1998.

[20] N. G. R. Broderick, T. M. Monro, P. J. Bennett, and D. J. Richardson, "Nonlinearity in holey optical fibers: measurement and future opportunities," Optics Letters, 24(20), 1395–1397, 1999.

[21] J. C. Knight, J. Arriaga, T. A. Birks, A. Ortigosa-Blanch, W. J. Wadsworth, and P. S. Russell, "Anomalous dispersion in photonic crystal fiber," IEEE Photonics Technology Letters, 12(7), 807–809, 2000.

[22] A. Ferrando, E. Silvestre, J. J. Miret, and P. Andres, "Nearly zero ultra flattened dispersion in photonic crystal fibers," Optics Letters, 25(11), 790–792, 2000.

[23] W. H. Reeves, D. V. Skryabin, F. Biancalana, J. C. Knight, P. S. Russell, F. G. Omenetto, A. Efimov, and A. J. Taylor, "Transformation and control of ultra-short pulses in dispersion-engineered photonic crystal fibers," Nature, 424(6948), 511–515, 2003.

[25] J. C. Knight, J. Broeng, T. A. Birks, and P. S. J. Russel, "Photonic band cap guidance in optical fibers," Science, 282(5393), 1476–1478, 1998.

[26] S. M. Sze, "Semiconductor devices," physics and technology Wiley, New York, 2nd edition, 2002.

[27] C. Kittel, "Introduction to solid state physics," Wiley, New York, 7th edition, 1996.

[28] E. Yablonovitch, "Inhibited spontaneous emission in solid-state physics and electronics," Physical Review Letters, 58(20), 2059–2062, 1987.

[29] S. John, "Strong localization of photons in certain disordered dielectric superlattices," Physical Review Letters, 58(23), 2486–2489, 1987.

[30] S. John, "Electromagnetic absorption in a disordered medium near a photon mobility edge," Physical Review Letters, 53(22), 2169–2172, 1984.

[31] O. Painter, R. K. Lee, A. Scherer, A. Yariv, J. D. O'Brien, P. D. Dapkus, and I. Kim, "Two-dimensional photonic band-gap defect mode laser," Science, 284(5421), 1819–1821, 1999.

[32] J. D. Joannopoulos, Robert D. Meade, and Joshua N. Winn, "Photonic crystals: molding the flow of light," Princeton University Press, Princeton, N.J., 1995.

[33] H. P. Myers, "Introductory solid state physics," Taylor and Francis, London, 2nd edition, 1997.

[34] R.T. Bise and D.J. Trevor, "Sol-gel derived microstructured fiber: fabrication and characterization," Optical Fiber Communication Conference, 2005. Technical Digest. OFC/NFOEC, 3(3), 2005.

[35] K Mukasa, M. N. Petrovich, F. Poletti, A. Webb, J. Hayes, A. van Brakel, R. Amezcua-Correa, L. Provost, J.K. Sahu, P. Petropoulos, and D.J. Richardson, "Novel fabrication method of highly-nonlinear silica holey fibers," Lasers and Electro-Optics, 2006. (CLEO). Conference on, May 2006.

[36] X. Feng, T.M. Monro, V. Finazzi, R.C. Moore, K. Frampton, P. Petropoulos, and D.J. Richardson, "Extruded single mode, high-nonlinearity, tellurite glass holey fiber," Electronics Letters, 41(15), 835–837, July 2005.

[37] B. Temelkuran, S. D. Hart, G. Benoit, J. D. Joannopoulos, and Y. Fink, "Wavelength-scalable hollow optical fibers with large photonic bandgaps for CO2 laser transmission," Nature, 420(6916), 650–653, 2002.

[38] S. K. Varshney, M. P. Singh, and R. K. Sinha, "Propagation characteristics of photonic crystal fibers," Journal of Optical Communications, 24, 2002.

[39] Allan W. Snyder and John D. Love, "Optical waveguide theory," Chapman and Hall, London, New York, 1983.

[40] J. C. Knight, T. A. Birks, R. F. Cregan, P. S. Russell, and J. P. de Sandro, "Large mode area photonic crystal fiber," Electronics Letters, 34(13), 1347–1348, 1998.

[41] W. J.Wadsworth, R. M. Percival, G. Bouwmans, J. C. Knight, and P. S. J. Russel, "High power air-clad photonic crystal fiber laser," Optics Express, 11(1), 48–53, 2003.

[42] J. Limpert, T. Schreiber, S. Nolte, H. Zellmer, A. Tunnermann, R. Iliew, F. Lederer, J. Broeng, G. Vienne, A. Petersson, and C. Jakobsen, "High-power air-clad large-mode-area photonic crystal fiber laser," Optics Express, 11(7), 818–823, 2003.

[43] W. H. Reeves, J. C. Knight, P. S. J. Russell, and P. J. Roberts, "Demonstration of ultra-flattened dispersion in photonic crystal fiber," Optics Express, 10(14), 609–613, 2002.

[44] Z. Yusoff, J. H. Lee, W. Belardi, T. M. Monro, P. C. Teh, and D. J. Richardson, "Raman effects in a highly nonlinear holey fiber: amplification and modulation," Optics Letters, 27(6), 424–426, 2002.

[45] J. E. Sharping, M. Fiorentino, P. Kumar, and R. S. Windeler, "All-optical switching based on cross-phase modulation in microstructure fiber," IEEE Photonics Technology Letters, 14(1), 77–79, 2002.

[46] P. Petropoulos, T. M. Monro, W. Belardi, K. Furusawa, J. H. Lee, and D. J. Richardson, "2R-regenerative all-optical switch based on a highly nonlinear holey fiber," Optics Letters, 26(16), 1233–1235, 2001.

[47] J. E. Sharping, M. Fiorentino, P. Kumar, and R. S. Windeler, "Optical parametric oscillator based on four-wave mixing in microstructure fiber," Optics Letters, 27(19), 1675–1677, 2002.

[48] X. Liu, C. Xu, W. H. Knox, J. K. Chandalia, B. J. Eggleton, S. G. Kosinski, and R. S. Windeler, "Soliton self-frequency shift in a short tapered air-silica microstructure fiber," Optics Letters, 26(6), 358–360, 2001.

[49] M. Fiorentino, J. E. Sharping, P. Kumar, A. Porzio, and R. S. Windeler, "Soliton squeezing in microstructure fiber," Optics Letters, 27(8), 649–651, 2002.

[50] J. Herrmann, U. Griebner, N. Zhavoronkov, A. Husakou, D. Nickel, J. C. Knight, W. J. Wadsworth, P. S. J. Russell, and G. Korn, "Experimental evidence for super continuum generation by fission of higher-order solitons in photonic fibers," Physical Review Letters, 88(17), 173901, 2002.

[51] A. V. Husakou and J. Herrmann, “Supercontinuum generation of higher-order solitons by fission in photonic crystal fibers,” Physical Review Letters, 8720(20), 203901, 2001.

[52] W. J. Wadsworth, A. Ortigosa-Blanch, J. C. Knight, T. A. Birks, T. P. M. Man, and P. S. Russell, “Supercontinuum generation in photonic crystal fibers and optical fiber tapers: a novel light source,” Journal of the Optical Society of America B Optical Physics, 19(9), 2148–2155, 2002.

[53] S. Coen, A. H. L. Chan, R. Leonhardt, J. D. Harvey, J. C. Knight, W. J. Wadsworth, and P. S. J. Russell, “White-light super continuum generation with 60-ps pump pulses in a photonic crystal fiber,” Optics Letters, 26(17), 1356–1358, 2001.

[54] A. Bjarklev, J. Broeng, S. Barkou, and A. S. Bjarklev, “Photonic Crystals Fibers,” Klumeer Academic Publishers, Boston, MA., 2003.

[55] F. Zolla, G. Renversez, A. Nicolet, B. Kuhlmey, S. Guenneau, and D. Felbacq, “Foundations of Photonic Crystals Fibers,” Imperial College Press, London, UK., 2005.

[56] Z. Zhang and S. Satpathy, “Electromagnetic-wave propagation in periodic structures bloch wave solution of maxwell equations,” Physical Review Letters, 65(21), 2650–2653, 1999.

[57] K. M. Ho, C. T. Chan, and C. M. Soukoulis, “Existence of a photonic gap in periodic dielectric structures,” Physical Review Letters, 65(25), 3152–3155, 1990.

[58] A. A. Maradudin and A. R. Mcgurn, “Out-of-plane propagation of electromagnetic waves in a 2-dimensional periodic dielectric medium,” Journal of Modern Optics, 41(2), 275–284, 1994.

[59] P. R. Villeneuve and M. Piche, “Photonic band-gaps in 2-dimensional square and hexagonal lattices,” Physical Review B, 46(8), 4969–4972, 1992.

[60] J. B. Pendry, “Photonic band structures,” Journal of Modern Optics, 41(2), 209–229, 1994.

[61] R. D. Meade, A. M. Rappe, K. D. Brommer, J. D. Joannopoulos, and O. L. Alerhand, “Accurate theoretical-analysis of photonic band-gap materials,” Physical Review B, 48(11), 8434 -8437, 1993.

[62] G. J. Pearce, T. D. Hedley, and D. M. Bird, “Adaptive curvilinear coordinates in a plane-wave solution of Maxwell’s equations in photonic crystals,” Physical Review B, 71(19), 2005.

[63] J. Broeng, S. E. Barkou, T. Sondergaard, and A. Bjarklev, "Analysis of air-guiding photonic bandgap fibers," Optics Letters, 25(2), 96–98, 2000.

[64] M. J. Steel, T. P. White, C. M. de Sterke, R. C. McPhedran, and L. C. Botten, "Symmetry and degeneracy in microstructured optical fibers," Optics Letters, 26(8), 488–490, 2001.

[65]http://www.google.co.in/search?hl=en&safe=active&q=Introduction+to+Chromatic+Dispersion&oq=Introduction+to+Chromatic+Dispersion&gs_l=serp.3..0i30.132976.132976.0.134396.1.1.0.0.0.0.160.160.0j1.1.0...0.0.9aSS6deSxRA.

[66] Philip Russell, "Recent Advances in Photonic Crystal Fibers," 5th International Conference on Transparent Optical Networks, 1, 8, 2003.

[67] Frederic GEROME, Jean-huh AUGUSTE, Jean-Marc BLONDY, "Very high negative chromatic dispersion in a dual concentric core photonic crystal fiber," Conference Paper Optical Fiber Communication Conference (OFC), 2004.

[68] Knnimasa Saitoh and Masanori Koshiba, "Unique Dispersion Properties of Photonic Crystal Fibers," ICICS-PCM, 171-175, 2003

[69] F. Poli, A. Cucinotta, S. Selleri, and A. H. Bouk, "Tailoring of Flattened Dispersion in Highly Nonlinear Photonic Crystal Fibers," IEEE Photonics Technology Letters, 16(4), 1065-1067, 2004

[70] Takashi Matsui, Jian Zhou, Kazuhide Nakajima, and Izumi Sankawa, "Dispersion-Flattened Photonic Crystal Fiber with Large Effective Area and Low Confinement Loss," Journal of Lightwave Technology, 23(12), 4178-4183, 2005

[71] Arismar Cerqueira S. Jr.* and K. Z. Nobregat, "Chromatic dispersion management of high-index glass photonic crystal fiber," International Conference on Microwave and Optoelectronics, 83-86, 2005

[72] Niels Asger Mortensen, "Photonic crystal fibers: mapping Maxwell's equations onto a Schrödinger equation eigen value problem," Physics Optics, 1-16, 2006

[73] Kudlinski, A.; George, A.K.; Knight, J.C., "Dispersion decreasing photonic crystal fiber for UV-enhanced super continuum generation." IEEE Conference Publications on Digest of the LEOS Summer Topical Meetings, 54-55, 2006.

[74] Federica Poli, Annamaria Cucinotta, Matteo Foroni, Stefano Selleri, "Finite-Element Based Photonic Crystal Fiber Analysis: From Solid to Hollow Core Fibers," IEEE/LEOS Winter Topical Meeting Series, 158-159, 2008.

[75] Sh. Mohammad Nejad, M. Aliramezani, M. Pourmahyabadi, "A Novel Design of Photonic Crystal Fiber with Ultra-Flattened Dispersion and Ultra-Low Loss," 4th IEEE/IFIP International Conference on Internet, 1-5, 2008.

[76] Takashi Matsui, Kazuhide Nakajima, and C. Fukai, "Applicability of Photonic Crystal Fiber with Uniform Air-Hole Structure to High-Speed and Wide-Band Transmission over Conventional Telecommunication Bands," Journal of Lightwave Technology, 27(23), 5410-5416, 2009.

[77] Nihal F. F. Areed land Hamdy Elmikati, "Ultra-Flattened Dispersion Photonic Crystal Fiber," 26th National Radio Science Conference, 1-10, 2009

[78] Uma R. Rao, B. K. Lande, "Photonic Crystal Fiber as Dispersion Compensator," International Conference on Advances in Computing, Communication and Control, 217-219, 2009

[79] Mohamed Farhat O. Hameed, Salah S. A. Obayya, Khalid Al-Begain, Moheb I. Abo el Maaty, and Abed M. Nasr, "Modal Properties of an Index Guiding Nematic Liquid Crystal Based Photonic Crystal Fiber," Journal of Lightwave Technology, 27(21), 4754-4762, 2009.

[80] S Arismar Cerqueira Jr, "Recent progress and novel applications of photonic crystal fibers," Reports on Progress in Physics, 73(02), 1-21, 2010.

[81] Sandhir K Singh, Dharmendra K Singh, P Mahto, **"**Design and Analysis of a 2D-Photonic Crystal Fiber Structure with Ultra-Flattened Dispersion and Single Mode Operation over a Wide Range of Wavelength," Journal of Advanced Networking and Applications, 1(5), 337-340, 2010.

[82] Saeed Olyaee and Fahimeh Taghipour, "A new design of photonic crystal fiber with ultra-flattened dispersion to simultaneously minimize the dispersion and confinement loss," Journal of Physics: Conference Series, 276(1), 1-6, 2011.

[83] Nagesh Janrao, Vijay Janyani, "Dispersion Compensation Fiber using Square Hole PCF," International Conference on Communications and Signal Processing (ICCSP), 436-438, 2011.